7-2017

The tension-sensitive ion transport activity of MSL8 is critical for its function in pollen hydration and germination

Eric S. Hamilton
Washington University in St. Louis

The Tension-sensitive Ion Transport Activity of MSL8 is Critical for its Function in Pollen Hydration and Germination

Running title:

Ion transport is required for MSL8 pollen function

Corresponding author: Dr. E. S. Haswell

Department of Biology, Box 1137, Washington University in St. Louis, One Brookings Drive, Saint Louis, MO, 63130, USA.

314-935-9223

ehaswell@wustl.edu

Subject areas: growth and development; membrane and transport

1 black and white figure; 7 color figures; 3 tables; 4 supplementary figures and 4 supplementary tables

16 **The Tension-sensitive Ion Transport Activity of MSL8 is Critical for its Function in Pollen Hydration**
17 **and Germination**
18
19 Running title:
20 Ion transport is required for MSL8 pollen function
21
22 Eric S. Hamilton and Elizabeth S. Haswell
23 Department of Biology, Box 1137, Washington University in St. Louis, One Brookings Drive, Saint Louis,
24 MO, 63130, USA.
25
26 Abbreviations: cRNA, capped RNA; MS, mechanosensitive; MscL, Mechanosensitive channel of Large
27 conductance; MscS, Mechanosensitive channel of Small conductance; MSL8, MscS-Like 8; MSL10; MscS-
28 Like 10; PEG, polyethylene glycol; TM, transmembrane

Abstract

All cells respond to osmotic challenges, including those imposed during normal growth and development. Mechanosensitive (MS) ion channels provide a conserved mechanism for regulating osmotic forces by conducting ions in response to increased membrane tension. We previously demonstrated that the MS ion channel MscS-Like 8 (MSL8) is required for pollen to survive multiple osmotic challenges that occur during the normal process of fertilization, and that it can inhibit pollen germination. However, it remained unclear whether these physiological functions required ion flux through a mechanically gated channel provided by MSL8. We introduced two point mutations into the predicted pore-lining domain of MSL8 that disrupted normal channel function in different ways. The Ile711Ser mutation increased the tension threshold of the MSL8 channel while leaving conductance unchanged, and the Phe720Leu mutation severely disrupted the MSL8 channel. Both of these mutations impaired the ability of MSL8 to preserve pollen viability during hydration and to maintain the integrity of the pollen tube when expressed at endogenous levels. When overexpressed in a *msl8-4* null background, $MSL8^{I711S}$ could partially rescue loss-of-function phenotypes, while $MSL8^{F720L}$ could not. When overexpressed in the wild type L*er* background, $MSL8^{I711S}$ suppressed pollen germination, similar to wild type MSL8. In contrast, $MSL8^{F720L}$ failed to suppress pollen germination and increased pollen bursting, thereby phenocopying the *msl8-4* mutant. Thus, an intact MSL8 channel is required to for normal pollen function during hydration and germination. These data establish MSL8 as the first plant MS channel to fulfill previously established criteria for assignment as a mechanotransducer.

Keywords: *Arabidopsis thaliana*; mechanosensitive ion channel; osmotic stress; pollen hydration; pollen germination

Introduction

In order to thrive, all cells must respond to osmotic challenges. Drought, salt stress, and freezing all present environmentally imposed stresses that require osmoprotective strategies for cell survival (Burg and Ferraris, 2008; Zhang, 1999). Organisms can also experience osmotic challenges inherent to their growth and development, such as desiccation during endospore formation in response to stress (Tovar-Rojo et al., 2003), the transition from seawater to saltwater experienced by migrating salmon (Jeffries et al., 2011), or drying and rehydration of plant seeds (Hoekstra et al., 2001).

One conserved molecular mechanism for responding to osmotic challenges and other mechanical stimuli is the use of mechanosensitive (MS) ion channels (Booth and Blount, 2012; Hamilton et al., 2015b; Ranade et al., 2015). These proteins form pores in the cell membrane that open in response to mechanical stimulation, allowing ions to flow across the membrane down their electrochemical gradient. A role for MS ion channels in osmotic control has been well described in *Escherichia coli*, where the Mechanosensitive channel of Large conductance (MscL) and Mechanosensitive channel of Small conductance (MscS) are required for the cell to survive extreme hypoosmotic downshock, such as the transfer from 500 mM NaCl to distilled water (Levina et al., 1999). It is proposed that when cells are exposed to hypoosmotic shock, the resultant cell swelling and increase in membrane tension increase the open probability of both MscS and MscL. When open, these channels allow ions and other small osmolytes to flow out of the cell, reducing internal osmotic pressure and protecting the bacterium from lysis (Booth and Blount, 2012; Kung et al., 2010). Thus, bacterial MS ion channels are often referred to as osmotic pressure release valves.

*Ec*MscS is the founding member of a large family of conserved proteins found within prokaryotes, archaea, and many eukaryotes, including plants (Haswell, 2007; Kloda and Martinac, 2002; Koprowski and Kubalski, 2003; Levina et al., 1999; Malcolm and Maurer, 2012; Pivetti et al., 2003; Porter et al., 2009; Prole and Taylor, 2013). Crystal structures of MscS homologs from *E. coli* and *Helicobacter pylori* have shown that these proteins form homoheptamers (Bass et al., 2002; Lai et al., 2013; Steinbacher et al., 2007; Wang et al., 2008), but no structural information yet exists for eukaryotic MscS family members. Ten MscS homologs

77 are encoded in the *Arabidopsis thaliana* genome, named MscS-Like (MSL) 1-10 (Haswell, 2007). MSL
78 proteins localize to diverse cell compartments, including the mitochondria (Lee et al., 2016), plastids
79 (Haswell and Meyerowitz, 2006), and the plasma membrane (Hamilton et al., 2015a; Haswell et al., 2008;
80 Veley et al., 2014).
81
82 We recently showed that plasma membrane-localized MSL8 is required to protect pollen from osmotic
83 challenges during several steps in fertilization (Hamilton et al., 2015a). Pollen contains the male gametes
84 of flowering plants and is responsible for the delivery of two sperm cells to the female gametophyte in order
85 to produce the next generation (Hafidh et al., 2016). During key steps of desiccation, rehydration,
86 germination, and tube growth, pollen must regulate its osmotic potential to maintain the integrity of the cell
87 and achieve its reproductive function (Beauzamy et al., 2014; Chen et al., 2015; Feijo et al., 1995; Firon et
88 al., 2012; Sanati Nezhad et al., 2013).
89
90 Upon maturation, the pollen of most species of flowering plants desiccates (Franchi et al., 2011), a strategy
91 thought to maintain viability during exposure to the external environment (Firon et al., 2012). To protect
92 against the osmotic stress of this water loss, pollen accumulates sugars and other compatible osmolytes
93 that serve to stabilize cellular membranes and other biomolecules in the dry state (Hoekstra et al., 2001;
94 Pacini et al., 2006). When a desiccated pollen grain reaches the stigma, an organ of finger-like projections
95 atop the pistil, it is rehydrated by stigma cell exudate in a regulated process of pollen reception (Dresselhaus
96 and Franklin-Tong, 2013; Edlund, 2004; Samuel et al., 2009). The wet stigma of lily is coated in exudate,
97 which is about 10% carbohydrates (Labarca et al., 1970). The composition of the exudate produced in
98 species with dry stigmas, such as Arabidopsis, is unknown (Edlund, 2004), but must be hypoosmotic with
99 respect to the pollen cytoplasm in order to produce net hydration. The rehydration of desiccated pollen can
100 damage dry cellular membranes, which are more rigid and less able to accommodate hypoosmotic swelling
101 (Hoekstra et al., 2001; 1997), and this membrane damage can compromise pollen viability if hydration is
102 not properly regulated (van Bilsen et al., 1994).
103

Once a pollen grain is rehydrated, its metabolism is reactivated and it germinates a long extension that grows by turgor-driven cell expansion at the tip without further cell divisions, called a pollen tube (Beauzamy et al., 2014; Firon et al., 2012). Germination requires that the pollen grain establish and maintain turgor pressure at a level high enough to break through the tough pollen cell wall (Feijo et al., 1995). The rapid growth of the pollen tube is also driven by turgor pressure, which continuously expands new cell wall material delivered to the growing tip (Hill et al., 2012; Kroeger et al., 2011; Zerzour et al., 2009). Artificially increasing turgor pressure can lead to lysis, especially at the tip of the pollen tube (Benkert et al., 1997), and genetic lesions that increase turgor impair the ability of the pollen tube to reach the ovule and fertilize the egg cell (Chen et al., 2015). Conversely, growth conditions that reduce turgor halt pollen tube growth (Zerzour et al., 2009). In addition to turgor, pollen tubes must regulate the delivery of new cell wall material and cell wall composition in order to sustain growth while maintaining the integrity of the cell (Hill et al., 2012; Kroeger et al., 2011; Zerzour et al., 2009). These observations have led to the proposal that pollen grains utilize a mechanosensor to respond to changes in osmotic potential (Hill et al., 2012), and a role for MS ion channels in regulating ion fluxes at the dynamic pollen tube tip has been proposed for decades (Feijo et al., 1995).

MSL8 provides one mechanism for regulating these osmotic forces in pollen. The null *msl8-4* allele, a T-DNA insertion in the Landsberg *erecta* background, results in reduced viability when pollen is hydrated in distilled water (Hamilton et al., 2015a). This hydration viability defect can be rescued by supplementing hydration media with a 20% solution of polyethylene glycol (PEG); increasing the osmotic potential of the media reduces the hypoosmotic shock pollen experiences during hydration. We were unable to detect any defect in hydration rate nor in the final size of in vitro hydrated pollen, indicating that wild type and *msl8-4* pollen have a similar capacity to hydrate. This evidence suggests that MSL8 serves to protect desiccated pollen against the hypoosmotic shock of rehydration.

MSL8 also functions during pollen germination and tube growth. Turgor pressure is required for pollen grains to germinate, and for pollen tubes to grow (Feijo et al., 1995), but it must be controlled in order to

prevent bursting (Kroeger et al., 2011; Zerzour et al., 2009). MSL8 appears to be involved in this process, as *msl8-4* pollen germinates at a greater rate than wild type pollen, but bursts more frequently, consistent with elevated turgor pressure in the mutant pollen grains and germinating tubes (Hamilton et al., 2015a). Conversely, overexpressing MSL8 inhibits pollen germination, likely by reducing turgor pressure below the level needed for the nascent pollen tube to break through the pollen grain cell wall. Both loss-of-function mutations in the *MSL8* gene and overexpression of *MSL8* result in male fertility defects. Taken together, these data show that the proper expression level of MSL8 is essential for full reproductive success.

Thus, MSL8 is required to maintain proper osmotic pressure inside pollen, either during rehydration or during the turgor-driven germination and growth of a pollen tube. Because MSL8 forms a MS ion channel, we hypothesized that the flow of ions through the MSL8 pore in response to increases in membrane tension is critical for preventing lysis during hydration and germination, akin to the function of MscS in *E. coli*. However, it remained possible that the role of MSL8 in pollen survival is indirect. Indeed, close homolog MSL10 triggers programmed cell death signaling independent of its channel activity (Veley et al., 2014). Here we report the results of experiments aimed to determine if MSL8 requires an intact channel to achieve its function in pollen. To do so, we mutated the predicted pore of the MSL8 channel, identified lesions that affect channel behavior, and analyzed the ability of these mutants to function in pollen. Our results support a model wherein MSL8 regulates osmotic forces in pollen directly by transporting ions.

Results

Mutations in the predicted pore-lining domain of MSL8 alter its channel properties

In order to alter the channel properties of MSL8, we identified candidate amino acids for mutagenesis based alignment with *Ec*MscS. The predicted topology of a MSL8 monomer shown in Fig. 1A indicates a protein with 6 transmembrane (TM) helices and three soluble domains. The most C-terminal TM helix, TM6, contains sequence with modest homology to the pore-lining TM3 of *Ec*MscS (marked with a thick line in Fig. 1A and sequence shown in Fig. 1B).

In the *Ec*MscS channel, Leu105 and Leu109 from each of the seven monomers are proposed to form a hydrophobic seal in the closed channel that prevents the flow of ions across the pore (Anishkin and Sukharev, 2004; Bass et al., 2002; Steinbacher et al., 2007) (arrowheads, Fig. 1B). Mutations in nearby residues can result in decreased tension sensitivity, increased tension sensitivity, or reduced conductance (Belyy et al., 2010; Edwards et al., 2005; Rasmussen et al., 2015). To create MSL8 variants with altered channel properties, we replaced hydrophobic residues surrounding the presumptive hydrophobic seal with polar residues or smaller non-polar residues. Two mutants, Ile711 to Ser and Phe720 to Leu (asterisks, Fig. 1B) were selected for further study based on their ability to produce MS currents when expressed in *Xenopus laevis* oocytes (see below).

MSL8, *MSL8*^{I711S} and *MSL8*^{F720L} cRNAs were injected into *Xenopus* oocytes for analysis by single channel patch-clamp electrophysiology as previously described (Hamilton et al., 2015a; Maksaev and Haswell, 2015). Patches of plasma membrane were excised from oocytes 2 to 10 days after injection, and current measured over time as membrane tension in the patch was increased by applying suction through the pipette using a pressure-clamp controller. In symmetric 60 mM $MgCl_2$ + 5mM HEPES, oocytes expressing wild type *MSL8* cRNA exhibited tension-gated activity as expected (Fig. 1C, top left panel), as did oocytes injected with *MSL8*^{I711S} cRNA (Fig. 1C, top right panel). In the same system, *MSL8*^{F720L} cRNA produced MS currents that could not be resolved into unitary channel openings (Fig. 1C, bottom left panel; see Supplementary Fig. S1 for more examples of activity associated with *MSL8*^{F720L} cRNA), and no currents

were observed in water-injected oocytes (Fig. 1C, bottom right panel). 60 mM $MgCl_2$ was used to encourage high resistance seal formation and to inhibit endogenous *Xenopus laevis* MS channels. MS currents were observed in 23 of 26 patches pulled from oocytes injected with *MSL8* cRNA; 27 of 32 patches for *MSL8*^{I711S}; 20 out of 24 patches for *MSL8*^{F720L}; and in none of 26 patches from water-injected oocytes (Table 1). Under these conditions, the single-channel conductance of MSL8^{I711S} was indistinguishable from that of wild type MSL8 (Fig. 1D, Table 1). Without distinguishable individual gating events, we were unable to assess the single channel conductance of MSL8^{F720L}.

We were unable to calculate a midpoint gating tension, because membrane patches ruptured before current saturation, as previously observed for MSL10 expressed in *Xenopus* oocytes (Maksaev and Haswell, 2012). Instead, we estimated the tension sensitivity of each MSL8 variant, by recording the suction associated with the opening of the first channel and the closing of the last channel in each patch. Patch pipettes of size 3 ± 0.5 MOhm were used in all experiments to reduce variability in patch geometry. The negative pressure required to open the first channel in patches expressing wild type MSL8 was -18.0 ± 13.1 mmHg, while for MSL8^{I711S} it was -29.5 ± 11.7 mmHg (Table 1). While we were unable to identify discrete channel openings for MSL8^{F720L}, we estimated its tension threshold by determining the pressure required to produce visible MS currents, on average -61.2 ± 12.3 mmHg (Table 1). In summary, MSL8^{I711S} had the same conductance as wild type MSL8, but was significantly less tension-sensitive (required greater negative pressure to open). MSL8^{F720L} appears to be a severely disrupted channel, albeit one capable of conducting ions through its pore in response to extremely high membrane tension, approximately 3 times higher than that required to open wild type MSL8.

MSL8 channel mutants do not complement msl8-4 mutant phenotypes when expressed from genomic sequences.

To determine whether channel activity was required for MSL8 to protect pollen from osmotic challenges, we tested whether MSL8^{I711S} or MSL8^{F720L} could complement previously characterized *msl8-4* mutant defects. The entire genomic sequence containing the *MSL8* gene (from 588 bp upstream of the ATG to 759

bp downstream of the stop codon) was cloned into a binary expression vector and the coding sequence for GFP inserted just before the *MSL8* stop codon. This construct, termed gMSL8-GFP, rescues the in vitro hydration viability defect of *msl8-4* pollen (Hamilton et al., 2015a). MSL8 variants were produced by site-directed mutagenesis of gMSL8-GFP. *gMSL8-GFP*, *gMSL8^{I711S}-GFP* and *gMSL8^{F720L}-GFP* transgenes were introduced into the null *msl8-4* mutant background via Agrobacterium transformation. Lines expressing wild type and mutant versions of *gMSL8-GFP* were generated and screened for expression of *MSL8* variants in floral RNA. Two independent homozygous transgenic lines expressing *gMSL8^{I711S}-GFP* or *gMSL8^{F720L}-GFP* and a single control line expressing wild type *gMSL8-GFP* were selected for further analysis. All lines selected accumulated *MSL8* transcripts at levels equal to or greater than the wild-type L*er* (Fig. 2A). To confirm protein production, stability and subcellular localization, confocal images were taken of GFP signal in mature, desiccated pollen isolated from these lines. All five lines expressing *gMSL8-GFP* or variants in the *msl8-4* background exhibited GFP signal localized to both the plasma membrane and endomembrane compartments, as previously observed for MSL8-GFP (Fig. 2B; (Hamilton et al., 2015a). Untransformed *msl8-4* mutant pollen only exhibited autofluorescence of the cell wall.

To test the ability of MSL8^{I711S} and MSL8^{F720L} to protect *msl8-4* pollen from the hypoosmotic shock of rehydration, we quantified the viability of mature, desiccated pollen after rehydration in distilled water. Pollen was incubated in 30 µl water with 1 µg/ml fluorescein diacetate (FDA) and 0.5 µg/ml propidium iodide (PI). FDA stains live pollen, while PI marks the outer membrane and cell wall of intact pollen and only accumulates inside compromised pollen. In a rehydration time course from 30 to 120 minutes, as expected, L*er* pollen viability exceeded 80% at all time points, while *msl8-4* pollen exhibited less than 35% survival on average, and *msl8-4* pollen expressing wild type *gMSL8-GFP* exhibited wild-type survival at all time points (Fig. 3A). However, there were no differences between the viability of *msl8-4* pollen and *msl8-4* pollen expressing the *gMSL8^{I711S}-GFP* or *gMSL8^{F720L}-GFP* transgenes in water at 30, 60, or 120 minutes after hydration. Thus, neither MSL8^{I711S} nor MSL8^{F720L} could complement this *msl8-4* mutant phenotype.

To determine if MSL8^{I711S} or MSL8^{F720L} could protect *msl8-4* pollen from intermediate levels of hypoosmotic stress, we quantified pollen viability following a 30-minute incubation in a range of PEG_{3350} concentrations. Supplementing hydration media with 15% PEG_{3350} increased the average viability of *msl8-4* pollen from 30% to 79% (Fig. 3B). PEG supplementation also increased the survival rate of *msl8-4* pollen expressing *gMSL8^{I711S}-GFP* and *gMSL8^{F720L}-GFP*, to a degree that was indistinguishable from that of the mutant *msl8-4* pollen across all levels of PEG (Fig. 3B). Thus, the *gMSL8^{I711S}-GFP* and *gMSL8^{F720L}-GFP* transgenes did not alter the sensitivity of *msl8-4* pollen to rehydration, even when osmotic supplementation was used to reduce the severity of the osmotic downshock.

msl8-4 pollen survives hydration in germination media, as it contains osmolytes (580 mOsmol), but exhibits increased germination rates and pronounced bursting when germinated *in vitro* (Hamilton et al., 2015a). We therefore quantified the germination and bursting rates of *msl8-4* pollen expressing *gMSL8^{I711S}-GFP-* and *gMSL8^{F720L}-GFP*. After incubation in germination media for 6 hours, most L*er* pollen was ungerminated and intact; 8% was ungerminated and burst; 12% germinated and was intact; and 4% germinated and burst (Fig. 4, Supplementary Table S1). *msl8-4* pollen germinated at a similar rate to L*er*, but 37% of ungerminated mutant pollen grains burst. Most of the *msl8-4* pollen that did germinate went on to burst, leaving only 49% intact pollen (compared to 89% for the wild type). While *msl8-4* pollen expressing *gMSL8-GFP* barely germinated or burst at all (< 0.5%) under these conditions, pollen expressing *gMSL8^{I711S}-GFP* or *gMSL8^{F720L}-GFP* had germination and bursting rates similar to *msl8-4* pollen. We thus found no evidence that MSL8^{I711S} or MSL8^{F720L} could substantially rescue known *msl8-4* loss-of-function phenotypes (Figs. 3-4), even though these variants were expressed at or above native levels and localized normally (Fig. 2).

MSL8^{I711S} but not MSL8^{F720L} partially rescues msl8-4 loss-of-function phenotypes when overexpressed.

To determine if we could detect partially functional channels if they were present at high levels, MSL8, MSL8^{I711S} or MSL8^{F720L} were tagged at the C-terminus with YFP and expressed under the control of the strong, pollen-specific promoter *LAT52* in the *msl8-4* background. We identified multiple independent homozygous lines that exhibited a range of transgene expression levels in floral RNA, from 1.9- to 9.6-fold

over the levels of endogenous *MSL8* in L*er* (Fig. 5A). YFP signal in *msl8-4* pollen expressing *LAT52pMSL8-YFP* and variants localized to the plasma membrane and endomembrane compartments of mature pollen (Fig. 5B; Supplementary Fig. S2A), and the intensity of YFP signal correlated with transcript level as revealed by RT-PCR (compare Fig. 5A and Supplementary Fig. S2A).

Pollen from L*er* and *msl8-4* lines overexpressing MSL8, MSL8^{I711S}, and MSL8^{F720L} was incubated in distilled water for 30 or 120 minutes and viability quantified as in Fig. 3. All three *msl8-4* + *LAT52pMSL8-YFP* lines survived as well as wild-type pollen at both time points, while the viability of *msl8-4* pollen expressing *LAT52pMSL8^{F720L}-YFP* was indistinguishable from that of *msl8-4* in all three independent lines (Fig. 6). Thus, even at high levels of expression, *MSL8^{F720L}* was unable to protect pollen from the hypoosmotic shock of rehydration. However, pollen from three *msl8-4* + *LAT52pMSL8^{I711S}-YFP* lines exhibited intermediate levels of pollen viability when hydrated in water. The level of protection was correlated with the level of *MSL8^{I711S}* expression in each line. Two independent lines, I711S-7 and I711S-12, exhibited averages of 44% to 63% survival during the time course. At both time points, I711S-7- and I711S-12 pollen viability was statistically significantly different from L*er*, *msl8-4*, and the other transgenic lines, representing an intermediate phenotype. The strongest-expressing line, I711S-4 (Fig. 5A), exhibited wild-type pollen viability at both 30 and 120 minutes. Thus, MSL8^{I711S} is able to partially rescue the *msl8-4* hydration viability defect when moderately overexpressed, while sufficiently high levels of expression fully complement the mutant phenotype.

Next, we incubated pollen from *msl8-4* + *LAT52pMSL8-YFP* and variant lines in germination media for 6 hours and quantified germination and bursting rates (Fig. 7A). As expected, expression of *LAT52pMSL8-YFP* suppressed both germination and bursting rates of *msl8-4*, to less than 1%, while expression of *LAT52pMSL8^{F720L}-YFP* did not (Fig. 7A, Supplementary Table S2). As with pollen rehydration, overexpression of *MSL8^{I711S}* in the *msl8-4* background resulted in partial rescue of the loss-of-function phenotypes. Depending on the line, mutant pollen expressing *LAT52pMSL8^{I711S}-YFP* germinated an average of 0% to 17%, and burst on average 4% to 36% of the time (much lower than the approximately

283 25% germination and 50% bursting of *msl8-4*). Both germination and bursting rates were inversely
284 correlated to the level of *MSL8* accumulation in the *LAT52pMSL8^{I711S}-YFP* line (compare Figs. 5A and 7A).
285 The pattern of bursting and germination in the highest expressing line, I711S-4, was statistically
286 indistinguishable from line WT-11 (Supplementary Table S2), indicating that MSL8^{I711S} can fully
287 complement when highly overexpressed.
288
289 Because germination is suppressed so strongly by *MSL8* overexpression, we also incubated pollen in
290 germination media for an extended period of time (overnight, or 16 hours), in order to maximize the number
291 of germination events (Fig. 7B-C, Supplementary Fig. S2B). Under these conditions, 63% of *msl8-4* pollen
292 germinated on average, compared to 44% of L*er* pollen. The overexpression of *MSL8-YFP* in the *msl8-4*
293 background strongly suppressed pollen germination, while the overexpression of *MSL8^{F720L}-YFP* did not.
294 The germination rate of *msl8-4* pollen was partially suppressed by expressing *LAT52pMSL8^{I711S}-YFP*, with
295 the strongest-expressing line, I711S-4, germinating 22% of the time and I711S-7 and I711S-12 germinating
296 at rates comparable to L*er*. This indicates that overexpression of MSL8^{F720L} does not rescue the elevated
297 germination and bursting rate of *msl8-4* pollen, and overexpression of MSL8^{I711S} produces a partial
298 reduction in both bursting and germination rates.
299
300 We previously observed that overexpressing *MSL8* reduces pollen fertility, likely through the suppression
301 of germination (Hamilton et al., 2015a). This fertility defect can be observed as a reduction in the
302 transmission of the transgene from the hemizygous T1 generation to the segregating T2 generation, as
303 determined by resistance to the herbicide Basta, which is conferred by the transgene. As expected, three
304 lines expressing *LAT52pMSL8-YFP* in the *msl8-4* background exhibited a significant reduction in transgene
305 transmission, reducing Basta resistance from the expected 75% to around 65%. However, none of the lines
306 overexpressing *MSL8^{I711S}-YFP* or *MSL8^{F720L}-YFP* in the *msl8-4* background showed a significant deviation
307 from the expected rate of resistance (Table 2). This indicates that neither MSL8^{I711S} nor MSL8^{F720L} have an
308 effect on pollen fertility and suggests that the partial suppression of *in vitro* germination conferred by
309 overexpressing *MSL8^{I711S}-YFP* in the *msl8-4* background is insufficient to reduce pollen fertility *in vivo*.

Thus, while neither MSL8^{F720L} nor MSL8^{I711S} provide clear function in pollen when expressed at endogenous levels, MSL8^{I711S} can provide some function when expressed at high levels.

Overexpressing MSL8^{F720L} in wild-type pollen increases bursting, while overexpressing MSL8 and MSL8^{I711S} suppresses pollen germination.

We also investigated the function of MSL8^{I711S} and MSL8^{F720L} when overexpressed in the wild type background, rather than in the *msl8-4* background as above. Transgenic *LAT52pMSL8-YFP,* *LAT52pMSL8^{F720L}-YFP*, or *LAT52pMSL8^{I711S}-YFP* lines were selected wherein *MSL8* or *MSL8* variants were expressed at levels similar to or higher than the endogenous *MSL8* gene (Fig. 8A). Quantitative RT-PCR revealed that transcript levels of endogenous *MSL8* were not significantly different from L*er* in the transgenic lines (Fig. 8A, dark gray bars), while total *MSL8* transcripts were increased over endogenous levels between 1.3 and 4.3-fold (Fig. 8A, light gray bars).

Pollen from lines expressing *LAT52pMSL8-YFP* and *LAT52pMSL8^{I711S}-YFP* did not germinate at all after incubation in germination media for 6 hours, and the bursting rate of ungerminated pollen grains was reduced to less than 7% (Fig. 8B). The pattern of pollen germination and bursting was indistinguishable between line WT-10 and the three lines overexpressing *MSL8^{I711S}-YFP* as determined by a chi-squared test (Fig. 8B, Supplementary Table S3). However, L*er* pollen expressing *LAT52pMSL8^{F720L}-YFP* burst 46% to 54% of the time, comparable to the bursting rate of *msl8-4*. Thus, overexpressing *MSL8^{F720L}* in the wild-type background produced a dominant negative effect, phenocopying the *msl8-4* mutant bursting rate. This elevated bursting rate is likely caused by MSL8^{F720L} disrupting the native pool of MSL8 through the formation of heteromeric channels (see discussion).

When incubated in germination media overnight, pollen overexpressing MSL8^{F720L} in the L*er* background germinated at rates between that of L*er* and *msl8-4*, indicating that it had little, if any, effect (Fig. 8C). However, overexpressing MSL8^{I711S} in the wild type background resulted in a partial suppression of germination rates, to between 9% and 18%. While line I711S-2 had a germination rate that was

337 indistinguishable from the pollen overexpressing wild type MSL8, the other two independent lines produced
338 pollen germination rates that were both significantly lower than that of L*er* and significantly higher than L*er*
339 + *LAT52pMSL8-YFP* lines, representing an intermediate phenotype.
340
341 We also quantified the effect of *MSL8* overexpression on male fertility in these lines via the segregation of
342 resistance to Basta. Overexpressing *LAT52pMSL8-YFP* in the L*er* background reduced Basta resistance
343 in the segregating T2 generation from 75% to less than 65% (Table 3). One line expressing
344 *LAT52pMSL8^{I711S}-YFP* also exhibited a significant reduction in Basta resistance, to 59%, but all other MSL8
345 variant lines did not. This indicates that MSL8^{F720L} overexpression does not have an effect on pollen fertility,
346 and suggests that the partial suppression of *in vitro* pollen germination produced by overexpressing
347 *MSL8^{I711S}* has only a modest effect *in vivo*.

Discussion

The tension-sensitive ion transport activity of MSL8 is critical for its function in pollen.

A role for MS ion channels in the response of pollen to mechanical and osmotic challenges was proposed more than 20 years ago (Feijo et al., 1995). Such a role has been solidly established for the canonical MS ion channel from *E. coli*, MscS (Edwards et al., 2005; Levin and Blount, 2004; Levina et al., 1999; Miller, 2003; Sukharev et al., 1994), and an initial analysis suggested that a MscS homolog from Arabidopsis, MSL8, might as well (Hamilton et al., 2015a). In our previous study (Hamilton et al., 2015a), we found that *msl8-4* pollen does not survive the hypoosmotic shock of rehydration, germinates at higher rates than the wild type, and bursts more frequently—all suggesting that MSL8 is required for pollen to relieve excessive turgor pressure during fertilization. *MSL8* overexpression also leads to reduced germination rates and low fertility, probably because high levels of MSL8 leads to lower than normal turgor pressure within the pollen grain. We thus proposed that the levels of MSL8 must be carefully tuned in order to balance the need of pollen to protect against lysis during rehydration and germination, while maintaining sufficient turgor pressure for germination and pollen tube growth. These data are consistent with MSL8 directly mediating the flux of ions in order to control the osmotic potential of pollen. However, it remained possible that MSL8 could play an indirect role in pollen, perhaps signaling independently of ion flux like close homolog MSL10 (Veley et al., 2014). Here we used site-directed mutagenesis, electrophysiology, and physiological assays to determine if the critical function of the MS ion channel MSL8 during pollen hydration and germination is to mediate ion flux.

Disrupting normal channel function prevents MSL8 from complementing known msl8-4 null loss-of-function phenotypes.

We identified two point mutations that, when introduced into the presumptive pore-lining helix, altered MSL8 channel behavior without appreciably altering expression, stability, or subcellular localization (Figs. 1, 2, Table 1). MSL8^{I711S} required higher membrane tension to open than MSL8, but had wild-type conductance. While MSL8^{F720L} produced MS currents that were never observed in water-injected oocytes, they did not form the step-wise increase in current characteristic of individual channel gating events, instead appearing

as a flickering increase in current that disappeared immediately after suction was released. MSL8^{F720L} also required significantly higher membrane tension to open than MSL8 or MSL8^{I711S}.

Our finding that MSL8^{F720L} was unable to rescue *msl8-4* loss-of-function phenotypes either at native levels of expression (Figs. 2-4) or when overexpressed (Figs. 5-7) demonstrated that a functional channel is necessary for MSL8 to protect pollen from the osmotic stress it experiences during hydration and germination. This supports a model where MSL8 functions akin to MscS, acting as an osmotic pressure release valve (Booth and Blount, 2012), albeit during developmentally programmed osmotic challenges rather than in response to environmental swings in osmolarity. During pollen germination and tube growth, which are powered by internal turgor pressure (Benkert et al., 1997; Zerzour et al., 2009), pollen must have multiple mechanisms to ensure that internal pressure and growth rates do not overtake the delivery of cell wall materials to the growing tip or the strength of the cell wall itself (Hill et al., 2012; Kroeger et al., 2011; Zerzour et al., 2009); MSL8 appears to be one of those mechanisms.

Increasing the tension threshold of the MSL8 channel reduces its physiological activity in pollen.

MSL8^{I711S} could only protect pollen from the hypoosmotic shock of rehydration and maintain the integrity of the pollen tube when overexpressed, and did not suppress pollen germination as strongly as the wild type. (Figs. 6-8). We propose that the precise tension threshold and conductance characteristics of MSL8 are critical for its ability to balance the need of pollen to maintain sufficient turgor pressure for germination and pollen tube growth while protecting against lysis during rehydration and germination. According to this view, the elevated tension threshold of MSL8^{I711S} would both reduce its ability to protect pollen from bursting and prevent it from strongly suppressing germination when overexpressed.

Although the evidence described above is consistent with MSL8 functioning like an osmotic safety valve, we note that we cannot exclude the possibility that the ion flow across MSL8 could act as a biochemical signal that indirectly achieves the same function. It also remains formally possible, though unlikely, that the Ile711Ser or Phe720Leu mutations affect both the characteristics of the channel and the function of other

domains important for signaling independent of ion transport. Lesions in both the soluble N-terminus (Veley et al., 2014) and the soluble C-terminus (Zou et al., 2015) affect the cell death signaling function of MSL10, but lesions to the predicted pore-lining domain have not yet been tested. Future work will be required to understand how MSL8 functions alongside established ion channels and the tightly regulated ion fluxes that are essential for pollen germination and tube growth (Michard et al., 2009).

MSL8^{F720L} has reduced channel activity and can act as a dominant negative allele.

MSL8^{F720L} conducts ions through its pore, but appears unable to form a stable open state or to transition normally between non-conducting and conducting configurations. (Fig. 1B, bottom left panel, Supplementary Fig. S1, Table 1). The closed form of *Ec*MscS is proposed to involve close packing of small residues from adjoining pore-lining domains (Edwards et al., 2005). The substitution of large hydrophobic residues for Gly or Ala at these positions results in less stable open state configurations with higher tension thresholds, that at least superficially resemble MSL8^{F720L} (Edwards et al., 2005; Rasmussen et al., 2015; Wu et al., 2011). Alternating chains of small hydrophobic amino acids are not observed in the predicted pore-lining domain of MSL8 (Fig. 1B). Rather, a repeating pattern of large hydrophobic/polar residues in the predicted pore-lining domain is conserved among the seven Arabidopsis MscS homologs predicted to localize to the plasma membrane. These residues include three phenylalanines at positions 710, 720 and 727 (marked with arrowheads, Supplementary Fig. S3). The observed channel characteristics of MSL8^{F720L} suggest that the pairing of similarly sized residues in the pore-lining domains may be an important factor in maintaining the stability and normal function of both MscS and MSLs. Testing this idea will require additional study, in particular detailed structural information for the plasma membrane-localized MSLs.

Expressing *MSL8^{F720L}* in a wild type background, and therefore in the presence of a native pool of MSL8, phenocopies the *msl8-4* mutant with respect to germination rate and pollen tube bursting (Fig. 8B-C). Because MSLs are likely to form homomeric channels (Haswell et al., 2008; Peyronnet et al., 2008), this dominant negative effect may be caused by the formation of heteromeric channel complexes. According to this model, the instability caused by the Phe720Leu mutation is dominantly imparted to MSL8-MSL8^{F720L}

heteromeric channels, reducing the number of functional MSL8 channels available, and thereby producing pollen with characteristics similar to those from the loss-of-function *msl8-4* background. A similar effect was described for the *Caenorhabditis elegans* TRP-4 candidate MS ion channel (Kang et al., 2010). A TRP-4 mutant that did not form a functional channel on its own dominantly ablated channel function when co-expressed with wild type TRP-4 in touch-sensitive neurons. How many MSL8^{F720L} monomers are sufficient to disrupt the function of an otherwise wild type MSL8 channel is not yet known.

MSL8^{I711S} can complement the msl8-4 mutant only when overexpressed

MSL8 Ile711 aligns with Ala110 of *Ec*MscS (Fig. 1B), and a mutation in the neighboring residue, Leu111, produces a similar disruption in function. In *Ec*MscS, Leu111Ser is associated with a doubled tension threshold, and MscS^{L111S} is unable to protect *E. coli* against osmotic shock (Belyy et al., 2010). Leu111 is part of the proposed "tension-transmitting clutch" that allows *Ec*MscS to respond to increases in membrane tension through hydrophobic associations with the other TM helices. The substitution of a hydrophilic residue for a hydrophobic one may weaken these interactions. Our data presented here show that Ile711 may play a similar force-transmitting role in MSL8. Once open, MSL8^{I711S} appears to produce a normal pore, as its single-channel conductance was wild type.

There are several possible explanations for the ability of MSL8^{I711S} to partially rescue loss-of-function phenotypes at high levels of expression. First, the gating of a MS ion channel is a stochastic process centered on the average tension threshold (Hille, 1992). Increasing the population of MSL8^{I711S} channels in pollen would increase the number of channels available in the population to open at lower tensions, potentially to levels sufficient for protection against osmotic stress. Alternatively, MSL8 could participate in cooperative gating, the lowering of the average tension threshold as the number of channels embedded in the membrane increases. Biophysical modeling experiments with MscL show that local deformation of the lipid bilayer at the channel periphery caused by flattening during the transition to the open state could explain the energetics of cooperative gating (Haselwandter and Phillips, 2013; Ursell et al., 2007). While

455 flattening has not been observed for MscS family members, cooperative gating could occur through a
456 different mechanism.
457
458 Regardless of the mechanism, overexpressing MSL8^{I711S} appears to result in an effective lowering of the
459 membrane tension required for gating, increasing its ability to regulate osmotic potential in pollen. Lowering
460 the tension threshold could also explain the observation that overexpressing wild-type MSL8 in the L*er*
461 background suppresses pollen germination (Fig. 8B, (Hamilton et al., 2015a)). If overexpression results in
462 MSL8 channel activity at lower membrane tensions, then the critical turgor for germination might never be
463 reached. Pollen would then be stuck in a futile cycle of building pressure, relieving pressure, and building
464 it again. In support of this idea, we observed that pollen overexpressing MSL8 developed the larger and
465 more structured vacuole morphology resembling normally germinating pollen (Supplementary Fig. S4;
466 (Hicks et al., 2004; Wudick et al., 2014)), though it rarely went on to germinate. Additional work is needed
467 to determine if overexpressing MSL8^{I711S} lowers its effective tension threshold, and if so, to identify the
468 mechanism by which this occurs.
469
470 *MSL8 could contribute to established anion fluxes in pollen.*
471 As MSL8 has an approximately 6-fold preference for conducting Cl^- over Na^+ (Hamilton et al., 2015a), it
472 might contribute to the anion fluxes previously observed in rehydrating pollen and growing pollen tubes.
473 Pollen grains efflux Cl^- immediately after rehydration and for several minutes afterward, both in vitro and in
474 vivo (Breygina et al., 2009; 2012; Matveyeva et al., 2003). Although the efflux of Cl^- during rehydration could
475 be due in part to unregulated leakage through the plasma membrane as it reorganizes in the hydrated state
476 (Hoekstra et al., 1999; 1992), it is largely blocked by anion channel inhibitors (Breygina et al., 2009; 2012;
477 Matveeva et al., 2003), suggesting that the majority of Cl^- ions exiting the cell during rehydration do so
478 through channels.
479
480 During pollen tube growth, chloride efflux at the tip oscillates along with growth rate (Zonia et al., 2001;
481 2002). Pharmacological inhibition of Cl^- efflux disrupts pollen tube growth, increases the volume of the tube

apex, and frequently induces pollen tube bursting at the tip (Breygina et al., 2009; Zonia et al., 2001; 2002), implicating this Cl^- flux in the control of osmotic potential. More recent studies have supported a role for Ca^{2+}-regulated Cl^- channels in these fluxes (Gutermuth et al., 2013; Tavares et al., 2011b), but MSL8 may contribute to the net Cl^- flux through a membrane tension-regulated, rather than Ca^{2+}-regulated, pathway.

We note that an electrophysiological survey in lily failed to find Cl^- channels of any kind in pollen grain protoplasts, and MS cation channel activity was only observed after extended incubation in pollen germination media (Dutta and Robinson, 2004). This discrepancy could be due to the limitations of the cell-attached electrophysiological method (Tavares et al., 2011a), as we have observed a MS Cl^- channel active in pollen protoplasts (Hamilton et al., 2015a).

MSL8 fulfills all criteria for assignment as a mechanotransducer.

The four criteria necessary for establishing a protein as the transducer of a physiological mechanical response are: (1) it is expressed in the correct cell and subcellular location to respond to mechanical stimulation; (2) it is required for the mechanosensory response, not the normal development of the cell; (3) it forms a MS channel in a heterologous system; and (4) structural changes that affect the protein's response in a heterologous system affect its function *in vivo* (Arnadottir and Chalfie, 2010). MscL and MscS in bacteria fulfill these criteria (Edwards et al., 2005; Levin and Blount, 2004; Levina et al., 1999; Miller, 2003; Sukharev et al., 1994), and NOMPC of *Drosophila* was recently shown to be a mechanotransducer of touch response in touch-sensitive neurons (Gong et al., 2013; Yan et al., 2013).

MSL8 now fulfills all four criteria: (1) it is expressed in tricellular and mature pollen and pollen tubes, and localizes to the plasma membrane; (2) it is not required for the normal development of pollen, but is required for protection against osmotic stress; (3) it forms a MS channel in the heterologous *Xenopus* oocyte system; and (4) altering its structure changes its electrophysiological characteristics and its physiological function, without affecting expression or subcellular localization.

Pollen faces additional, relatively unstudied mechanical challenges during its development, and mechanically sensitive proteins are likely to be involved. Desiccation is critical for the success of pollen from most species (Franchi et al., 2011), and presents unique osmotic and mechanical challenges (Firon et al., 2012; Hoekstra et al., 1997; 2001). Furthermore, as it invades the sporophytic tissue to reach the female gametophyte, the pollen tube must sense, produce, and regulate the forces required to grow in between other cells (Sanati Nezhad et al., 2013). Finally, the regulated process of bursting that must occur to release the sperm cells from within the pollen tube represents a fascinating case where mechanisms that previously maintained the structural integrity of the cell must be overcome in order to complete fertilization (Amien et al., 2010; Dresselhaus et al., 2016; Woriedh et al., 2013). Using electrophysiology, mutagenesis and physiological assays, we discovered that mechanosensitive ion channels are one mechanism pollen relies on to respond to the mechanical effects of osmotic changes. This powerful combination of techniques, as well as the development of new tools to probe pollen in the dry state, may uncover other mechanical and ionic regulation strategies in pollen and other plant cells.

522 **Materials and Methods**

523

524 *Plant material and growth conditions.* Plants were grown on soil under 24 hours of light at 21°C. *msl8-4*
525 (DsLoxN101568 and DsLoxN101751, in the L*er* background) was obtained from the Arabidopsis Biological
526 Resource Center. MSL8^{I711S} and MSL8^{F720L} constructs were produced through site-directed mutagenesis
527 from existing vectors (described in (Hamilton et al., 2015)) and transformed into *msl8-4* or L*er* by floral dip.

528

529 *Multiple alignments*. Alignments were performed in MEGA7 using a Clustal alignment with a pairwise
530 alignment gap opening penalty of 10 and gap extension penalty of 0.1 and a multiple alignment gap opening
531 penalty of 10 and gap extension penalty of 0.2. Sequences for alignment were based on previous
532 phylogenetic analysis of *Ec*MscS and Arabidopsis MSLs (Haswell, 2007) predicting the pore-lining domains
533 of MSLs based on the known pore-lining domain of *Ec*MscS.

534

535 *Electrophysiology.* Single channel patch-clamp electrophysiology was performed as described in (Maksaev
536 and Haswell, 2015). Capped RNA (cRNA) of *MSL8* was transcribed *in vitro* using the mMESSAGE
537 mMACHINE SP6 kit (Ambion) and stored at 1μg/μl at -80 °C. Defolliculated oocytes were purchased from
538 Xenopus1 (Dexter, MI) and injected with 50 nl of cRNA or water and patched in symmetric 60 mM $MgCl_2$
539 after incubating for 2-10 days in ND96 buffer + gentamycin.

540

541 *Reverse-transcriptase-polymerase chain reaction.* RNA was isolated from floral tissue (stage 13/14 flowers)
542 using the Qiagen RNeasy Mini RNA extraction kit (Qiagen). cDNA was generated from 2 μg RNA using an
543 oligo(dT)$_{20}$ primer and the M-MLV Reverse Transcriptase kit (Promega). *ACTIN,* total *MSL8,* endogenous
544 *MSL8* and *MSL8-YFP* transcripts were amplified with the primers listed in Supplementary Table S4 using
545 SYBR Green PCR Master Mix (Applied Biosciences) and 0.25 μL cDNA at a final volume of 25 μL.
546 Quantitative RT-PCR was performed using the StepOnePlus real-time PCR system (Applied Biosystems).
547 Total *MSL8* was amplified using primers that do not distinguish between the endogenous locus and the

548 transgenes. Endogenous *MSL8* was amplified using a reverse primer in the 3' UTR, which is not present in
549 the transgenes.
550
551 *In vitro pollen hydration.* Pollen from mature (stage 13-14) flowers was hydrated in 25-30 µl drops of water
552 or the indicated percentage of PEG (average molecular weight 3350 g/mol, Sigma-Aldrich) at a final
553 concentration of 1 µg/ml fluorescein diacetate (FDA, Sigma-Aldrich) and 0.5 µg/ml propidium iodide (PI,
554 Sigma-Aldrich) on double-ring cytology slides. Slides were inverted and incubated in a humid chamber at
555 room temperature for the indicated amount of time. To image, cover slips were added and FDA signal was
556 collected in the GFP epifluorescence channel while PI signal was collected in the dsRed epifluorescence
557 channel. FDA stains live pollen while PI enters dead pollen.
558
559 *In vitro pollen germination.* Pollen germination was performed according to (Daher, Chebli, Geitmann 2009
560 Plant Cell Rep). Pollen was pre-hydrated by removing flowers from plants and incubating for 45 minutes at
561 30°C in a humid chamber constructed from a large petri dish containing smaller petri dishes placed on top
562 of moistened filter paper. Pollen was incubated in 30 µl of pollen germination media (2 mM $CaCl_2$, 2 mM
563 $Ca(NO_3)_2$, 0.49 mM H_3BO_3, 1 mM $MgSO_4$, 1 mM KCl, 18% w/v sucrose, pH 7) at 30°C for 6 or 16 hours in
564 a humid chamber as during pollen hydration. Pollen was counted as germinated if it had produced a pollen
565 tube longer than the pollen grain. Pollen was counted as burst if expelled cytoplasm was visible outside the
566 pollen grain or pollen tube.
567
568 *Microscopy*. Confocal images of GFP or YFP signal in pollen were acquired on an Olympus BX-61
569 microscope using FV10-ASW Olympus software and the GFP (488 nm excitation, 505-605 nm bandpass
570 filter) or YFP (515 nm excitation, 535-565 nm bandpass filter) channels. Brightfield and epifluorescent
571 images for pollen germination and pollen viability assays were collected on the same microscope using an
572 Olympus DP71 digital camera, DP Controller software, and filter sets for GFP (470/40 nm excitation, 525/50
573 nm emission) or dsRED (545/30 nm excitation, 620/60 nm emission).
574

Calculation of transmission ratios. The transmission frequencies of the *MSL8* transgenes were determined by selecting seedlings from the T2 generation with Basta on soil and counting the number of sensitive and resistant progeny. The Basta resistance gene *bar* is included in the transgene.

Statistical analyses. One-way or two-way ANOVAs were performed as indicated in figure legends. Tukey's HSD post-hoc test was used to determine statistical significance for balanced data sets. Scheffe's post-hoc test was used to determine statistical significance for unbalanced data sets. Chi-squared tests with Bonferroni correction were performed for analysis of transgene transmission and for comparison between groups of the pattern of germinated and burst pollen during pollen germination assays.

Funding

This study was funded by NSF MCB1253103 to E. S. Haswell and by the Monsanto Excellence Fund Fellowship to E. S. Hamilton.

Disclosures

The authors have no conflicts of interest to declare.

Acknowledgements

We thank G. Maksaev for advice and assistance. We acknowledge the Washington University plant growth facility for their assistance.

References

Amien, S., Kliwer, I., Márton, M.L., Debener, T., Geiger, D., Becker, D., and Dresselhaus, T. (2010). Defensin-like ZmES4 mediates pollen tube burst in maize via opening of the potassium channel KZM1. PLoS Biology *8*, e1000388.

Anishkin, A., and Sukharev, S. (2004). Water Dynamics and Dewetting Transitions in the Small Mechanosensitive Channel MscS. Biophysical Journal *86*, 2883–2895.

Arnadottir, J., and Chalfie, M. (2010). Eukaryotic mechanosensitive channels. Annual Review of Biophysics *39*, 111–137.

604 Bass, R.B., Strop, P., Barclay, M., and Rees, D.C. (2002). Crystal structure of Escherichia coli MscS, a
605 voltage-modulated and mechanosensitive channel. Science *298*, 1582–1587.

606 Beauzamy, L., Nakayama, N., and Boudaoud, A. (2014). Flowers under pressure: ins and outs of turgor
607 regulation in development. Annals of Botany *114*, 1517–1533.

608 Belyy, V., Anishkin, A., Kamaraju, K., Liu, N., and Sukharev, S. (2010). The tension-transmitting “clutch”
609 in the mechanosensitive channel MscS. Nat Struct Mol Biol *17*, 451–458.

610 Benkert, R., Obermeyer, G., and Bentrup, F.-W. (1997). The turgor pressure of growing lily pollen tubes.
611 Protoplasma *198*, 1–8.

612 Booth, I.R., and Blount, P. (2012). The MscS and MscL families of mechanosensitive channels act as
613 microbial emergency release valves. J. Bacteriol. *194*, 4802–4809.

614 Breygina, M.A., Matveeva, N.P., and Ermakov, I.P. (2009). The role of Cl– in pollen germination and tube
615 growth. Russ J Dev Biol *40*, 157–164.

616 Breygina, M.A., Matveyeva, N.P., Andreyuk, D.S., and Yermakov, I.P. (2012). Transmembrane transport
617 of K+ and Cl– during pollen grain activation in vivo and in vitro. *43*, 85–93.

618 Burg, M.B., and Ferraris, J.D. (2008). Intracellular organic osmolytes: function and regulation. J. Biol.
619 Chem. *283*, 7309–7313.

620 Chen, L.-Y., Shi, D.-Q., Zhang, W.-J., Tang, Z.-S., Liu, J., and Yang, W.-C. (2015). The Arabidopsis
621 alkaline ceramidase TOD1 is a key turgor pressure regulator in plant cells. Nature Communications *6*,
622 6030.

623 Dresselhaus, T., and Franklin-Tong, N. (2013). Male-female crosstalk during pollen germination, tube
624 growth and guidance, and double fertilization. Molecular Plant *6*, 1018–1036.

625 Dresselhaus, T., Sprunck, S., and Wessel, G.M. (2016). Fertilization Mechanisms in Flowering Plants.
626 Current Biology *26*, R125–R139.

627 Dutta, R., and Robinson, K.R. (2004). Identification and Characterization of Stretch-Activated Ion
628 Channels in Pollen Protoplasts. *135*, 1398–1406.

629 Edlund, A.F. (2004). Pollen and Stigma Structure and Function: The Role of Diversity in Pollination. The
630 Plant Cell *16*, S84–S97.

631 Edwards, M.D., Li, Y., Kim, S., Miller, S., Bartlett, W., Black, S., Dennison, S., Iscla, I., Blount, P., Bowie,
632 J.U., et al. (2005). Pivotal role of the glycine-rich TM3 helix in gating the MscS mechanosensitive channel.
633 Nat Struct Mol Biol *12*, 113–119.

634 Feijo, J.A., Malh, R., and Obermeyer, G. (1995). Ion dynamics and its possible role during in vitro pollen
635 germination and tube growth. Protoplasma *187*, 155–167.

636 Firon, N., Nepi, M., and Pacini, E. (2012). Water status and associated processes mark critical stages in
637 pollen development and functioning. Annals of Botany *109*, 1201–1214.

638 Franchi, G.G., Piotto, B., Nepi, M., Baskin, C.C., Baskin, J.M., and Pacini, E. (2011). Pollen and seed
639 desiccation tolerance in relation to degree of developmental arrest, dispersal, and survival. Exbotj *62*,
640 5267–5281.

641 Gong, J., Wang, Q., and Wang, Z. (2013). NOMPC is likely a key component of
642 Drosophilamechanotransduction channels. Eur J Neurosci *38*, 2057–2064.

643 Gutermuth, T., Lassig, R., Portes, M.T., Maierhofer, T., Romeis, T., Borst, J.W., Hedrich, R., Feijo, J.A.,
644 and Konrad, K.R. (2013). Pollen Tube Growth Regulation by Free Anions Depends on the Interaction
645 between the Anion Channel SLAH3 and Calcium-Dependent Protein Kinases CPK2 and CPK20. *25*,
646 4525–4543.

647 Hafidh, S., Fíla, J., and Honys, D. (2016). Male gametophyte development and function in angiosperms: a
648 general concept. Plant Reproduction 1–21.

649 Hamilton, E.S., Jensen, G.S., Maksaev, G., Katims, A., Sherp, A., and Haswell, E.S. (2015a).
650 Mechanosensitive channel MSL8 regulates osmotic forces during pollen hydration and germination.
651 Science *350*, 438–441.

652 Hamilton, E.S., Schlegel, A.M., and Haswell, E.S. (2015b). United in Diversity: Mechanosensitive Ion
653 Channels in Plants. Annu. Rev. Plant Biol.

654 Haselwandter, C.A., and Phillips, R. (2013). Directional interactions and cooperativity between
655 mechanosensitive membrane proteins. Europhys Lett *101*, 68002p1–68002p6.

656 Haswell, E.S. (2007). MscS-Like Proteins in Plants. *58*, 329–359.

657 Haswell, E.S., and Meyerowitz, E.M. (2006). MscS-like Proteins Control Plastid Size and Shape in
658 Arabidopsis thaliana. Current Biology *16*, 1–11.

659 Haswell, E.S., Peyronnet, R., Barbier-Brygoo, H., Meyerowitz, E.M., and Frachisse, J.-M. (2008). Two
660 MscS Homologs Provide Mechanosensitive Channel Activities in the Arabidopsis Root. Current Biology
661 *18*, 730–734.

662 Hicks, G.R., Rojo, E., Hong, S., Carter, D.G., and Raikhel, N.V. (2004). Geminating pollen has tubular
663 vacuoles, displays highly dynamic vacuole biogenesis, and requires VACUOLESS1 for proper function.
664 Plant Physiology *134*, 1227–1239.

665 Hill, A.E., Shachar-Hill, B., Skepper, J.N., Powell, J., and Shachar-Hill, Y. (2012). An Osmotic Model of
666 the Growing Pollen Tube. PLoS ONE *7*, e36585.

667 Hille, B. (1992). Ionic Channels of Excitable Membranes (Sunderland, Massachusetts: Sinauer
668 Associates Incorporated).

669 Hoekstra, F.A., Golovina, E.A., Aelst, A.C.V., and Hemminga, M.A. (1999). Imbibitional leakage from
670 anhydrobiotes revisited. Plant, Cell & Environment *22*, 1121–1131.

671 Hoekstra, F.A., Crowe, J.H., and Crowe, L.M. (1992). Germination and ion leakage are linked with phase
672 transitions of membrane lipids during imbibition of Typha latifolia pollen. Physiol Plantarum *84*, 29–34.

673 Hoekstra, F.A., Golovina, E.A., and Buitink, J. (2001). Mechanisms of plant desiccation tolerance. Trends
674 in Plant Science *6*, 431–438.

675 Hoekstra, F.A., Wolkers, W.F., Buitink, J., Golovina, E.A., Crowe, J.H., and Crowe, L.M. (1997).
676 Membrane Stabilization in the Dry State. Comparative Biochemistry and Physiology Part a: Physiology
677 *117*, 335–341.

678 Jeffries, K.M., Hinch, S.G., Donaldson, M.R., Gale, M.K., Burt, J.M., Thompson, L.A., Farrell, A.P.,
679 Patterson, D.A., and Miller, K.M. (2011). Temporal changes in blood variables during final maturation and
680 senescence in male sockeye salmon Oncorhynchus nerka: reduced osmoregulatory ability can predict
681 mortality. J. Fish Biol. *79*, 449–465.

682 Kang, L., Gao, J., Schafer, W.R., Xie, Z., and Xu, X.Z.S. (2010). C. elegans TRP Family Protein TRP-4 Is
683 a Pore-Forming Subunit of a Native Mechanotransduction Channel. Neuron *67*, 381–391.

684 Kloda, A., and Martinac, B. (2002). Common evolutionary origins of mechanosensitive ion channels in
685 Archaea, Bacteria and cell-walled Eukarya. Archaea *1*, 35–44.

686 Koprowski, P., and Kubalski, A. (2003). C Termini of the Escherichia coli Mechanosensitive Ion Channel
687 (MscS) Move Apart upon the Channel Opening. J. Biol. Chem. *278*, 11237–11245.

688 Kroeger, J.H., Zerzour, R., and Geitmann, A. (2011). Regulator or Driving Force? The Role of Turgor
689 Pressure in Oscillatory Plant Cell Growth. PLoS ONE *6*, e18549.

690 Kung, C., Martinac, B., and Sukharev, S. (2010). Mechanosensitive channels in microbes. Annu. Rev.
691 Microbiol. *64*, 313–329.

692 Labarca, C., Kroh, M., and Loewus, F. (1970). The Composition of Stigmatic Exudate from Lilium
693 longiflorum: Labeling Studies with Myo-inositol, D-Glucose, and L-Proline. Plant Physiology *46*, 150–156.

694 Lai, J.Y., Poon, Y.S., Kaiser, J.T., and Rees, D.C. (2013). Open and shut: Crystal structures of the
695 dodecylmaltoside solubilized mechanosensitive channel of small conductance from Escherichia coliand
696 Helicobacter pyloriat 4.4 Å and 4.1 Å resolutions. Protein Science *22*, 502–509.

697 Lee, C.P., Maksaev, G., Jensen, G.S., Murcha, M.W., Wilson, M.E., Fricker, M., Hell, R., Haswell, E.S.,
698 Millar, A.H., and Sweetlove, L. (2016). MSL1 is a mechanosensitive ion channel that dissipates
699 mitochondrial membrane potential and maintains redox homeostasis in mitochondria during abiotic stress.
700 Plant J.

701 Levin, G., and Blount, P. (2004). Cysteine Scanning of MscL Transmembrane Domains Reveals
702 Residues Critical for Mechanosensitive Channel Gating. Biophysical Journal *86*, 2862–2870.

703 Levina, N., Tötemeyer, S., Stokes, N.R., Louis, P., Jones, M.A., and Booth, I.R. (1999). Protection of
704 Escherichia coli cells against extreme turgor by activation of MscS and MscL mechanosensitive channels:
705 identification of genes required for MscS activity. The EMBO Journal *18*, 1730–1737.

706 Maksaev, G., and Haswell, E.S. (2015). Expressing and characterizing mechanosensitive channels in
707 Xenopus oocytes. Methods in Molecular Biology *1309*, 151–169.

708 Maksaev, G., and Haswell, E.S. (2012). MscS-Like10 is a stretch-activated ion channel from Arabidopsis
709 thaliana with a preference for anions. Proc Natl Acad Sci USA *109*, 19015–19020.

710 Malcolm, H.R., and Maurer, J.A. (2012). The Mechanosensitive Channel of Small Conductance (MscS)
711 Superfamily: Not Just Mechanosensitive Channels Anymore. ChemBioChem *13*, 2037–2043.

712 Matveeva, N.P., Andreyuk, D.S., Voitsekh, O.O., and Ermakov, I.P. (2003). Regulatory Changes in the
713 Intracellular pH and Cl– Efflux at Early Stages of Pollen Grain Germination in vitro. Russian Journal of
714 Plant Physiology *50*, 318–323.

715 Matveyeva, N.P., Andreyuk, D.S., and Yermakov, I.P. (2003). Transport of Cl– across the Plasma

716 Membrane during Pollen Grain Germination in Tobacco. Biochemistry (Moscow) *68*, 1247–1251.

717 Michard, E., Alves, F., and Feijo, J.A. (2009). The role of ion fluxes in polarized cell growth and
718 morphogenesis: the pollen tube as an experimental paradigm. *53*, 1609–1622.

719 Miller, S. (2003). Domain organization of the MscS mechanosensitive channel of Escherichia coli. The
720 EMBO Journal *22*, 36–46.

721 Pacini, E., Guarnieri, M., and Nepi, M. (2006). Pollen carbohydrates and water content during
722 development, presentation, and dispersal: a short review. Protoplasma *228*, 73–77.

723 Peyronnet, R., Haswell, E.S., Barbier-Brygoo, H., and Frachisse, J.-M. (2008). AtMSL9 and AtMSL10:
724 Sensors of plasma membrane tension in Arabidopsis roots. Plant Signaling & Behavior *3*, 726–729.

725 Pivetti, C.D., Yen, M.R., Miller, S., Busch, W., Tseng, Y.H., Booth, I.R., and Saier, M.H. (2003). Two
726 Families of Mechanosensitive Channel Proteins. Microbiology and Molecular Biology Reviews *67*, 66–85.

727 Porter, B.W., Zhu, Y.J., Webb, D.T., and Christopher, D.A. (2009). Novel thigmomorphogenetic
728 responses in Carica papaya: touch decreases anthocyanin levels and stimulates petiole cork outgrowths.
729 Annals of Botany *103*, 847–858.

730 Prole, D.L., and Taylor, C.W. (2013). Identification and Analysis of Putative Homologues of
731 Mechanosensitive Channels in Pathogenic Protozoa. PLoS ONE *8*, e66068–e66069.

732 Ranade, S.S., Syeda, R., and Patapoutian, A. (2015). Mechanically Activated Ion Channels. Neuron *87*,
733 1162–1179.

734 Rasmussen, T., Rasmussen, A., Singh, S., Galbiati, H., Edwards, M.D., Miller, S., and Booth, I.R. (2015).
735 Properties of the Mechanosensitive Channel MscS Pore Revealed by Tryptophan Scanning Mutagenesis.
736 Biochemistry *54*, 4519–4530.

737 Samuel, M.A., Chong, Y.T., Haasen, K.E., Aldea-Brydges, M.G., Stone, S.L., and Goring, D.R. (2009).
738 Cellular pathways regulating responses to compatible and self-incompatible pollen in Brassica and
739 Arabidopsis stigmas intersect at Exo70A1, a putative component of the exocyst complex. The Plant Cell
740 *21*, 2655–2671.

741 Sanati Nezhad, A., Naghavi, M., Packirisamy, M., Bhat, R., and Geitmann, A. (2013). Quantification of
742 cellular penetrative forces using lab-on-a-chip technology and finite element modeling. Proceedings of the
743 National Academy of Sciences of the United States of America *110*, 8093–8098.

744 Steinbacher, S., Bass, R., Strop, P., and Rees, D.C. (2007). Structures of the Prokaryotic
745 Mechanosensitive Channels MscL and MscS. In Mechanosensitive Ion Channels, Part A, (Elsevier), pp.
746 1–24.

747 Sukharev, S.I., Blount, P., Martinac, B., Blattner, F.R., and Kung, C. (1994). A large-conductance
748 mechanosensitive channel in E. coli encoded by mscL alone. Nature *368*, 265–268.

749 Tavares, B., Domingos, P., Dias, P.N., Feijo, J.A., and Bicho, A. (2011a). The essential role of anionic
750 transport in plant cells: the pollen tube as a case study. *62*, 2273–2298.

751 Tavares, B., Dias, P.N., Domingos, P., Moura, T.F., Feijó, J.A., and Bicho, A. (2011b). Calcium-regulated
752 anion channels in the plasma membrane of Lilium longiflorum pollen protoplasts. The New Phytologist
753 *192*, 45–60.

754 Tovar-Rojo, F., Cabrera-Martinez, R.-M., Setlow, B., and Setlow, P. (2003). Studies on the mechanism of
755 the osmoresistance of spores of Bacillus subtilis. J. Appl. Microbiol. *95*, 167–179.

756 Ursell, T., Huang, K.C., Peterson, E., and Phillips, R. (2007). Cooperative gating and spatial organization
757 of membrane proteins through elastic interactions. PLoS Comput Biol *3*, e81.

758 van Bilsen, D., Hoekstra, F.A., Crowe, L.M., and Crowe, J.H. (1994). Altered Phase Behavior in
759 Membranes of Aging Dry Pollen May Cause Imbibitional Leakage. Plant Physiology *104*, 1193–1199.

760 Veley, K.M., Maksaev, G., Frick, E.M., January, E., Kloepper, S.C., and Haswell, E.S. (2014). Arabidopsis
761 MSL10 has a regulated cell death signaling activity that is separable from its mechanosensitive ion
762 channel activity. The Plant Cell *26*, 3115–3131.

763 Wang, W., Black, S.S., Edwards, M.D., Miller, S., Morrison, E.L., Bartlett, W., Dong, C., Naismith, J.H.,
764 and Booth, I.R. (2008). The structure of an open form of an E. coli mechanosensitive channel at 3.45 A
765 resolution. Science *321*, 1179–1183.

766 Woriedh, M., Wolf, S., Márton, M.L., Hinze, A., Gahrtz, M., Becker, D., and Dresselhaus, T. (2013).
767 External application of gametophyte-specific ZmPMEI1 induces pollen tube burst in maize. Plant
768 Reproduction *26*, 255–266.

769 Wu, H.M., Hazak, O., Cheung, A.Y., and Yalovsky, S. (2011). RAC/ROP GTPases and auxin signaling.
770 The Plant Cell *23*, 1208–1218.

771 Wudick, M.M., Luu, D.T., Tournaire-Roux, C., Sakamoto, W., and Maurel, C. (2014). Vegetative and
772 sperm cell-specific aquaporins of Arabidopsis highlight the vacuolar equipment of pollen and contribute to
773 plant reproduction. Plant Physiology *164*, 1697–1706.

774 Yan, Z., Zhang, W., He, Y., Gorczyca, D., Xiang, Y., Cheng, L.E., Meltzer, S., Jan, L.Y., and Jan, Y.N.
775 (2013). Drosophila NOMPC is a mechanotransduction channel subunit for gentle-touch sensation. Nature
776 *493*, 221–225.

777 Zerzour, R., Kroeger, J., and Geitmann, A. (2009). Polar growth in pollen tubes is associated with
778 spatially confined dynamic changes in cell mechanical properties. Developmental Biology *334*, 437–446.

779 Zhang, J. (1999). Genetic analysis of osmotic adjustment in crop plants. Exbotj *50*, 291–302.

780 Zonia, L., Cordeiro, S., and Feijo, J.A. (2001). Ion dynamics and hydrodynamics in the regulation of pollen
781 tube growth. Sex Plant Reprod *14*, 111–116.

782 Zonia, L., Cordeiro, S., Tupý, J., and Feijo, J.A. (2002). Oscillatory Chloride Efflux at the Pollen Tube
783 Apex Has a Role in Growth and Cell Volume Regulation and Is Targeted by Inositol 3,4,5,6-
784 Tetrakisphosphate. *14*, 2233–2249.

785 Zou, Y., Chintamanani, S., He, P., Fukushige, H., Yu, L., Shao, M., Zhu, L., Hildebrand, D.F., Tang, X.,
786 and Zhou, J.-M. (2015). A gain-of-function mutation in Msl10 triggers cell death and wound-induced
787 hyperaccumulation of jasmonic acid in Arabidopsis. Journal of Integrative Plant Biology *58*, 600–609.

788

Tables

Table 1. Conductance, tension threshold, and number of observations of MSL8 variants in *Xenopus* oocytes

	Conductance	Tension Threshold		Patches with activity / total patches
		First channel to open, mmHg	Last channel to close, mmHg	
MSL8	60.0	-18.9 ± 13.1	-1.7 ± 3.5	23/26
MSL8^{I711S}	60.7	-29.5 ± 11.7	-9.4 ± 9.5	27/32
MSL8^{F720L}	NA	-61.2 ± 12.3	-52.7 ± 11.5	20/24
Water	NA	NA	NA	0/26

799 **Table 2. Transmission of *LAT52pMSL8-YFP* variant transgenes in the *msl8-4* background**

800

msl8-4 + LAT52pMSL8-YFP	T2 progeny resistant to Basta				
	Line	% Expected	% Observed (number observed/total)	X^2	p
MSL8	1	75	67.2 (86/128)	5.18	0.023
	14	75	66.1 (74/112)	5.79	0.016
	11	75	64.0 (80/125)	9.52	0.002
MSL8^{F720L}	1	75	78.3 (47/60)	0.23	0.64
	10	75	74.4 (29/39)	0.05	0.83
	2	75	75.9 (41/54)	0.01	0.94
MSL8^{I711S}	7	75	74.0 (91/12)	0.23	0.64
	12	75	76.7 (89/116)	0.07	0.79
	4	75	74.1 (86/116)	0.18	0.67

801 **Table 3. Transmission of *LAT52pMSL8-YFP* variant transgenes in the wild-type background**

802

		T2 progeny resistant to Basta			
L*er* + *LAT52pMSL8-YFP*	Line	% Expected	% Observed (number observed/total)	X^2	p
MSL8	10	75	60.0 (30/50)	6.00	0.014
	27	75	63.9 (53/83)	5.50	0.019
MSL8^{F720L}	5	75	78.9 (30/38)	0.32	0.57
	6	75	67.3 (66/98)	3.06	0.080
	9	75	76.9 (40/52)	0.10	0.75
MSL8^{I711S}	1	75	58.6 (34/58)	8.30	0.0040
	2	75	65.6 (40/61	2.89	0.089
	4	75	72.3 (34/47)	0.18	0.67

803 **Figure Legends**

804

805 **Figure 1. Mutations in the predicted pore-lining domain alter channel properties of MSL8.** (**A**)
806 Predicted topology of MSL8. N and C mark the amino- and carboxy-terminal ends respectively. Thick line
807 marks the predicted pore-lining domain. Residues mutated in this study are indicated. (**B**) Multiple alignment
808 of the predicted pore-lining transmembrane regions of Arabidopsis MSL8, Arabidopsis MSL10 and the
809 known pore-lining domain of *E. coli MscS*. Identical residues conserved in at least half of the sequences
810 are shaded darkly; similar residues conserved at this level are shaded in gray. Residues proposed to form
811 the channel seal in *Ec*MscS are marked with arrowheads. MSL8 residues mutated in this study are marked
812 with an asterisk. (**C**) Representative traces from excised inside-out patches of plasma membrane from
813 *Xenopus laevis* oocytes following injection with the indicated cRNA or water clamped at -40 mV membrane
814 potential. (**D**) The current-voltage relationship of MSL8 (squares, $N = 4$ oocytes) and MSL8^{I711S} (triangles,
815 $N = 9$ oocytes) in symmetric 60 mM $MgCl_2$. Dashed line indicates the slope from which the single-channel
816 conductance was measured (see Table 1). Error bars are mean ± SE.

817

818 **Figure 2. Expression and subcellular localization of MSL8-GFP expressed from endogenous**
819 **sequences**. (**A**) Quantitative reverse-transcription polymerase chain reaction amplification of *MSL8*
820 transcripts in L*er*, *msl8-4*, and *gMSL8-GFP* transgenic lines. Levels are presented relative to *ACTIN*.
821 Different letter groups indicate significant ($p < 0.05$) differences between groups as determined by Tukey's
822 post-hoc test following one-way ANOVA. Error bars are mean ± SE of three biological and two technical
823 replicates. (**B**) Confocal images of GFP signal in pollen from stage 13-14 flowers from the indicated lines
824 hydrated in water. Arrowheads mark GFP signal at the plasma membrane. Scale bar is 20 μm.

825

826 **Figure 3. MSL8^{I711S}-GFP and MSL8^{F720L}-GFP do not complement the *msl8-4* hydration viability defect**
827 **when expressed from endogenous sequences.** (**A**) Hydration viability time course. Mature, desiccated
828 pollen from *msl8-4* + gMSL8-GFP and variant lines hydrated in distilled water for the indicated periods of
829 time. Viability was determined by staining with fluorescein diacetate (which marks live pollen) and propidium

iodide (which enters compromised cells). The average of 3-6 experiments with $N = 58 – 377$ pollen grains per experiment is shown. (**B**) Hydration viability in PEG_{3350} series. The average of 3-9 experiments with $N = 68-566$ pollen grains per experiment is presented. Different letter groups indicate significant ($p < 0.05$) differences between groups as determined by Scheffe's post-hoc test following two-way ANOVA. Error bars are mean ± SE.

Figure 4. MSL8^{I711S}-GFP and MSL8^{F720L}-GFP do not suppress *msl8-4* pollen bursting or germination when expressed from endogenous sequences. Mature, desiccated pollen from the indicated lines were incubated in germination media for 6 hours then examined under the microscope. Each pollen grain scored was placed into one of the four indicated categories. Pollen was counted as germinated if it had produced a pollen tube longer than the pollen grain. Pollen was counted as burst if expelled cytoplasm was visible. Averages from 3-6 experiments with $N = 101-236$ pollen per experiment are presented. See Supplementary Table 1 for statistical differences between groups. Error bars are mean ± SE.

Figure 5. Expression and subcellular localization of MSL8^{I711S}-YFP and MSL8^{F720L}-YFP expressed from the *LAT52* promoter in the *msl8-4* background. (**A**) Quantitative reverse-transcription polymerase chain reaction amplification of *MSL8* transcripts, presented relative to *ACTIN*, in L*er*, *msl8-4*, and *msl8-4* + *LAT52pMSL8-YFP* transgenic lines. Error bars are mean ± SE. (**B**) Confocal images of YFP signal in *msl8-4* pollen or *msl8-4* pollen expressing *LAT52pMSL8-YFP*, *LAT52pMSL8^{I711S}-YFP*, or *LAT52pMSL8^{F720L}-YFP*. Arrowheads mark GFP signal at the plasma membrane. Arrowheads mark GFP signal at the plasma membrane. Note that the autofluorescent cell wall is only visible in untransformed *msl8-4* pollen, which was imaged at higher laser power than the transgenic lines. Scale bars are 20 μm.

Figure 6. MSL8^{I711S}-YFP but not MSL8^{F720L}-YFP partially rescues the *msl8-4* hydration viability defect when overexpressed in the *msl8-4* background. Hydration viability time course, performed as described in Fig. 3. The average of 3 to 4 experiments with $N = 124$ to 354 pollen per experiment is presented.

Different letter groups indicate significant ($p < 0.05$) differences between groups as determined by Scheffe's post-hoc test following two-way ANOVA. Error bars are mean ± SE.

Figure 7. MSL8^{I711S}-YFP but not MSL8^{F720L}-YFP partially suppresses *msl8-4* pollen bursting and germination when overexpressed in the *msl8-4* background. (**A**) Pollen from the indicated lines incubated in germination media for 6 hours and scored for combined germination and bursting categories as in Fig. 4. Average of 3 to 6 experiments with *N* = 107 to 512 pollen per experiment. See Supplementary Table 2 for statistical differences between groups. (**B**) Germination rate of pollen from the indicated lines after incubation in germination media for 16 hours. Different letter groups indicate significant ($p < 0.05$) differences between groups as determined by Tukey's post-hoc test following one-way ANOVA. (**C**) Brightfield images of pollen from the indicated lines after incubation for 16 hours in liquid germination media. Scale bars are 50 μm. (**A**, **B**) Error bars are mean ± SE.

Figure 8. Effect of overexpressing MSL8-YFP variants from the *LAT52* promoter in the wild type background on germination phenotypes. (**A**) Quantitative reverse-transcription polymerase chain reaction of endogenous *MSL8*, *MSL8-YFP*, and total *MSL8* transcripts relative to *ACTIN* in L*er*, *msl8-4*, and *LAT52pMSL8-YFP* transgenic lines. (**B**) Pollen from the indicated lines incubated in germination media for 6 hours and scored for combined germination and bursting categories as in Fig. 4. Averages from 3 experiments with *N* = 82 to 250 pollen per experiment are presented. See Supplementary Table 3 for statistical differences between groups. (**C**) Germination rate of pollen from the indicated lines after incubation in germination media for 16 hours. Averages of 3 experiments with *N* = 99 to 257 pollen per experiment are presented. Different letter groups indicate significant ($p < 0.05$) differences between groups as determined by Tukey's post-hoc test following one-way ANOVA. (**A**-**C**) Error bars are mean ± SE.

FIGURE 1

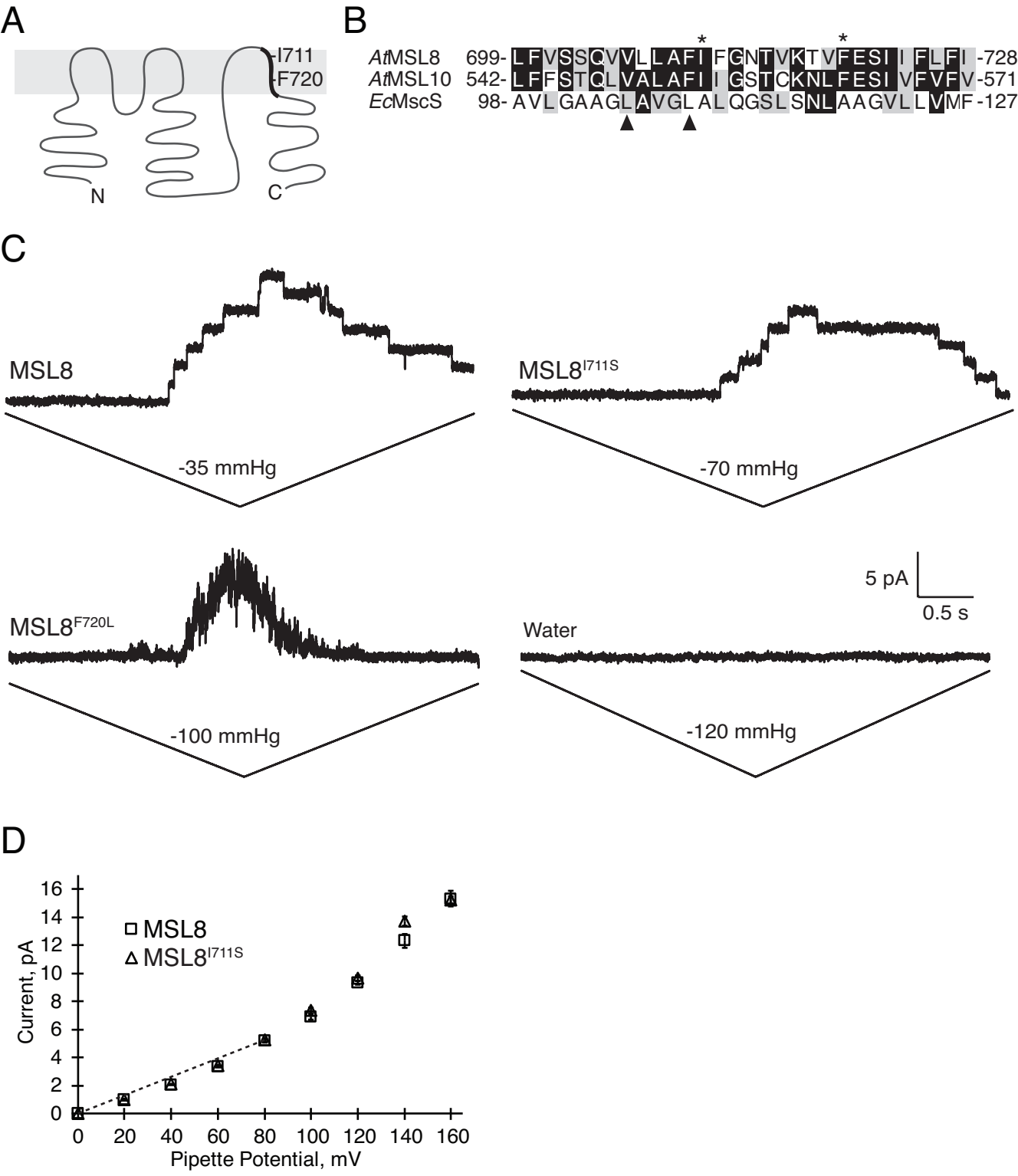
A
I711
F720
N
C
B
*
*
AtMSL8 699- LFVSSQVVLLAFIFGNTVKTVFESIIFLFI -728
AtMSL10 542- LFFSTQLVALAFIIGSTCKNLFESIVFVFV-571
EcMscS 98- AVLGAAGLAVGLALQGSLSNLAAGVLLVMF-127
C
MSL8
-35 mmHg
MSL8I711S
-70 mmHg
MSL8F720L
-100 mmHg
5 pA
0.5 s
Water
-120 mmHg
D
MSL8
MSL8I711S
Current, pA
Pipette Potential, mV
0
2
4
6
8
10
12
14
16
0
20
40
60
80
100
120
140
160

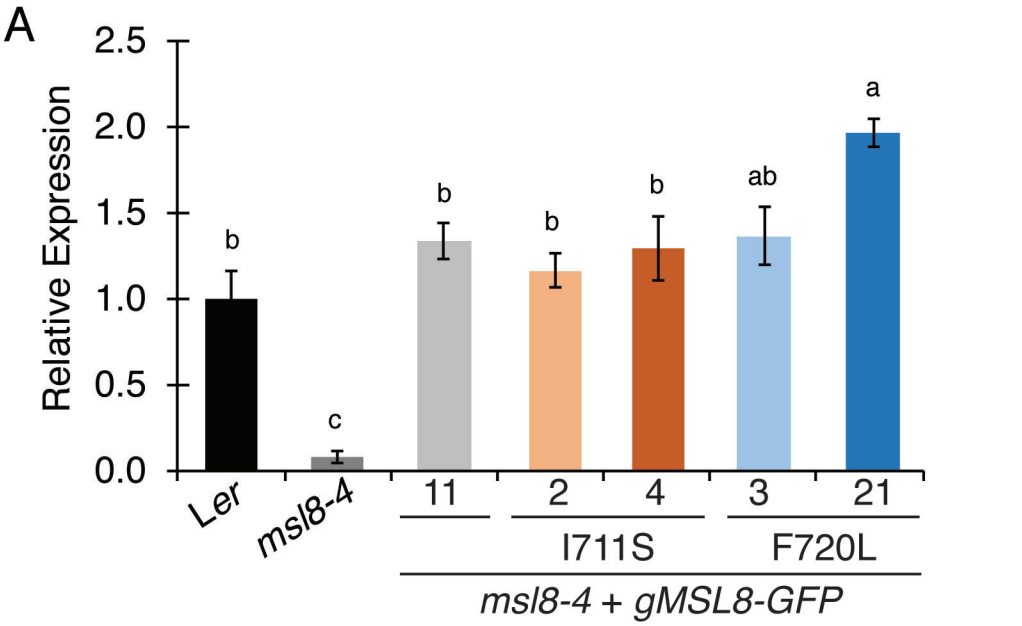
A
Relative Expression
2.5
2.0
1.5
1.0
0.5
0.0
b
c
b
b
b
ab
a
Ler
msl8-4
11
2
4
3
21
I711S
F720L
msl8-4 + gMSL8-GFP

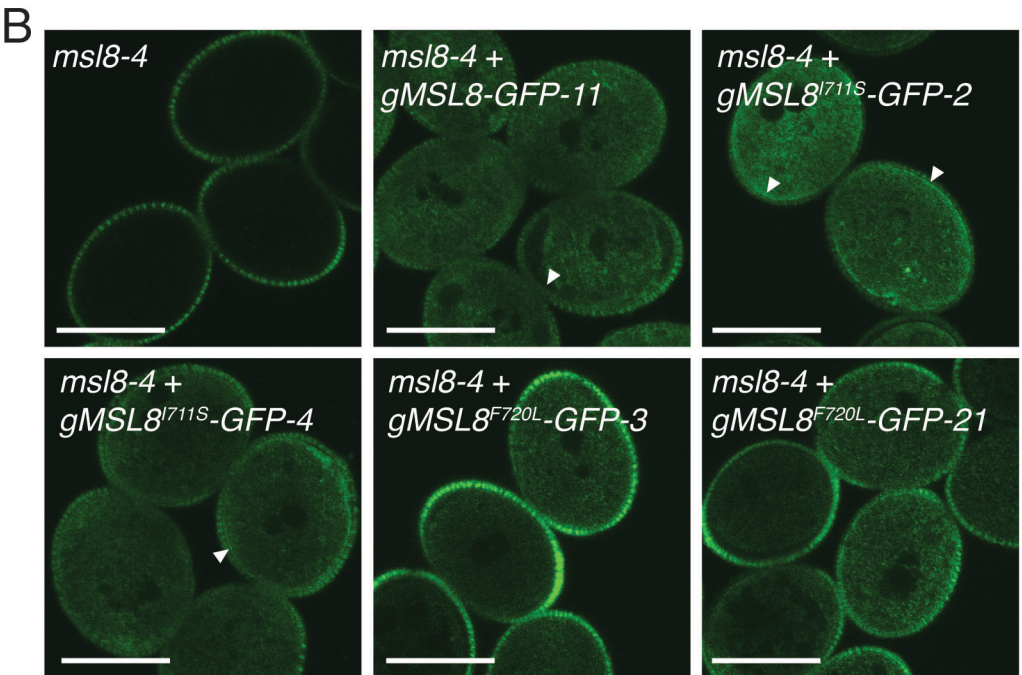
B
msl8-4
msl8-4 + gMSL8-GFP-11
msl8-4 + gMSL8I711S-GFP-2
msl8-4 + gMSL8I711S-GFP-4
msl8-4 + gMSL8F720L-GFP-3
msl8-4 + gMSL8F720L-GFP-21

FIGURE 3

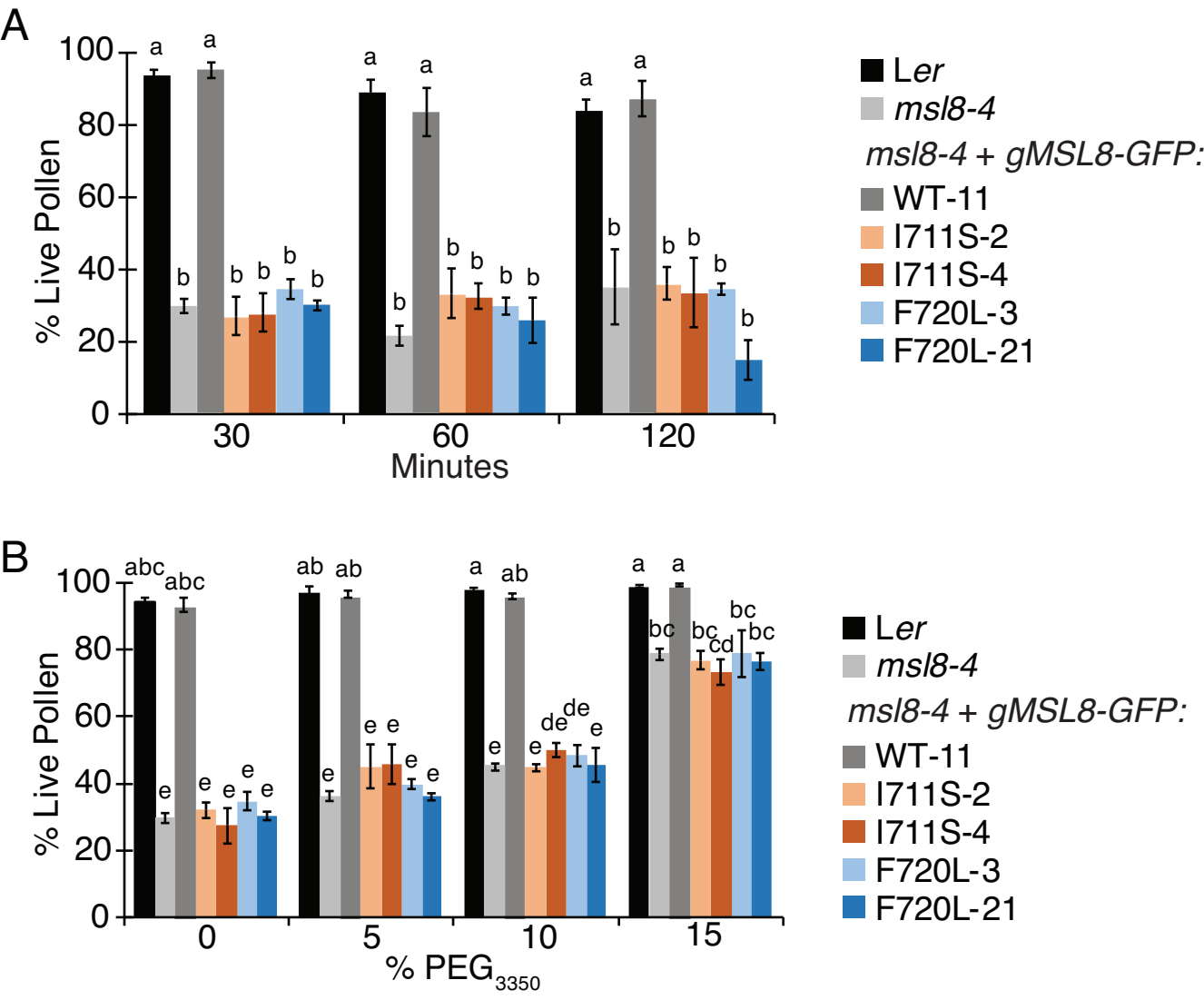
A
% Live Pollen
100
80
60
40
20
0
30
60
120
Minutes
Ler
msl8-4
msl8-4 + gMSL8-GFP:
WT-11
I711S-2
I711S-4
F720L-3
F720L-21
B
% Live Pollen
0
5
10
15
% PEG3350

FIGURE 4

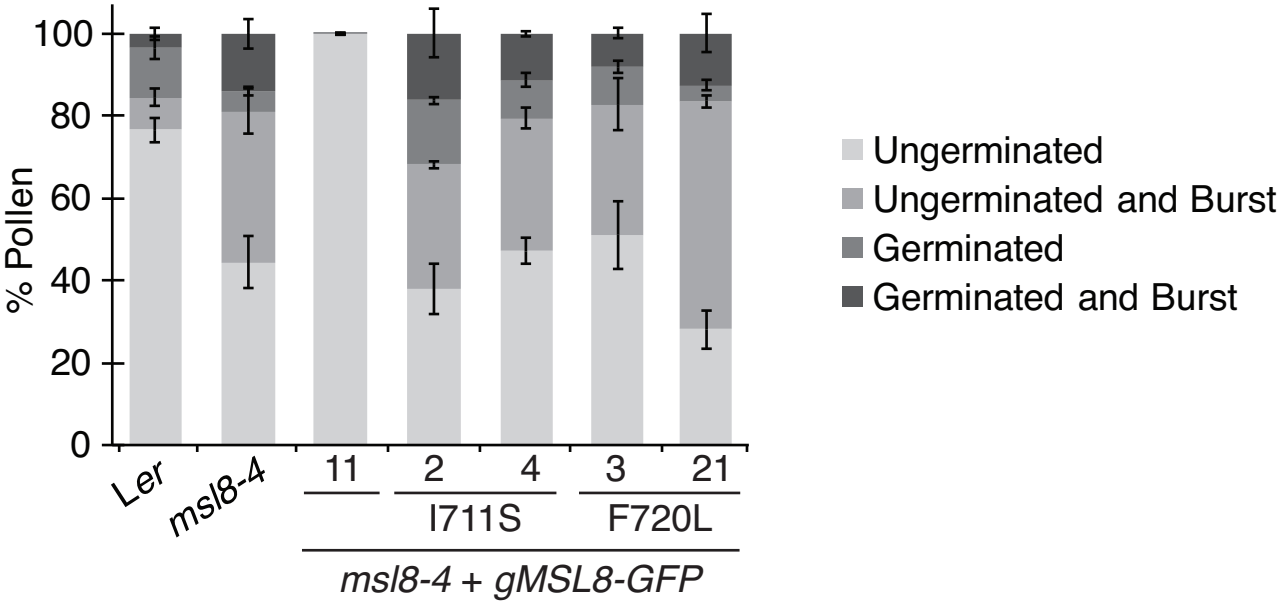
100
80
60
40
20
0
% Pollen
Ler
msl8-4
11
2
4
3
21
I711S
F720L
msl8-4 + gMSL8-GFP
Ungerminated
Ungerminated and Burst
Germinated
Germinated and Burst

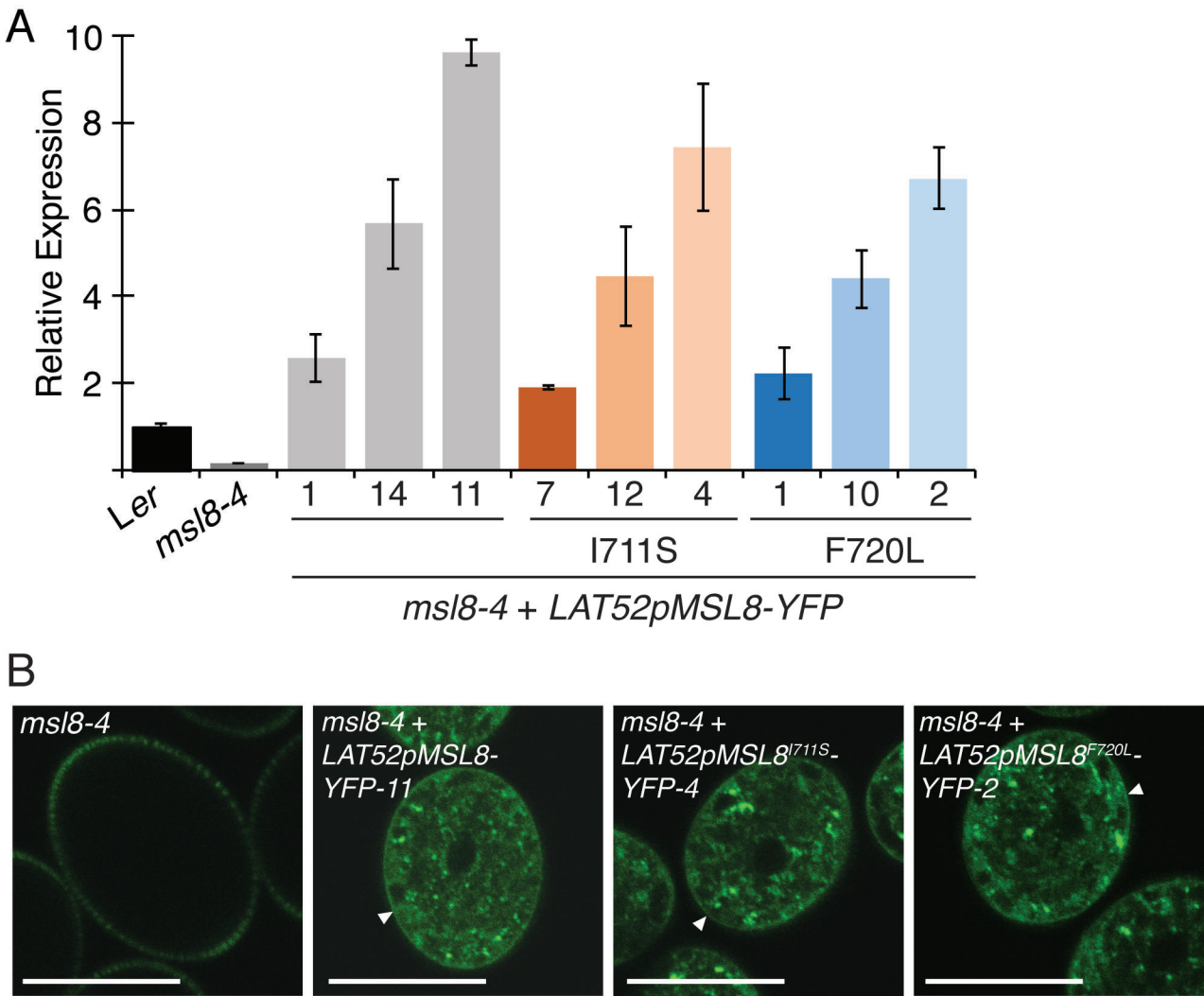
A
Relative Expression
10
8
6
4
2
Ler
msl8-4
1
14
11
7
12
4
1
10
2
I711S
F720L
msl8-4 + LAT52pMSL8-YFP
B
msl8-4
msl8-4 + LAT52pMSL8-YFP-11
msl8-4 + LAT52pMSL8I711S-YFP-4
msl8-4 + LAT52pMSL8F720L-YFP-2

FIGURE 6

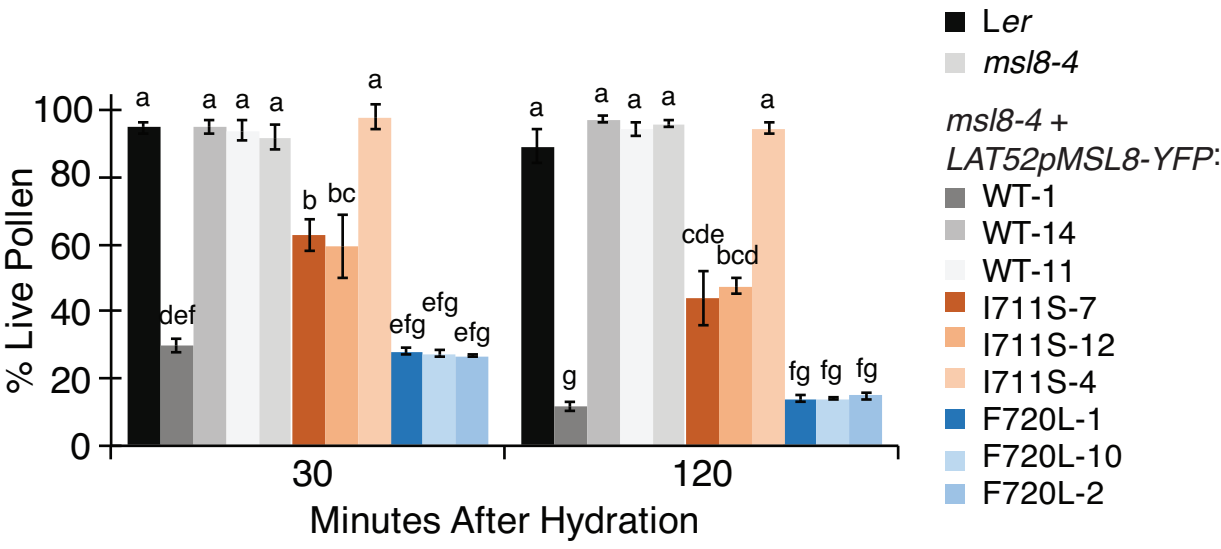
% Live Pollen
100
80
60
40
20
0
a
def
a
a
a
b
bc
a
efg
efg
efg
a
g
a
a
a
cde
bcd
a
fg
fg
fg
30
120
Minutes After Hydration
Ler
msl8-4
msl8-4 +
LAT52pMSL8-YFP:
WT-1
WT-14
WT-11
I711S-7
I711S-12
I711S-4
F720L-1
F720L-10
F720L-2

FIGURE 7

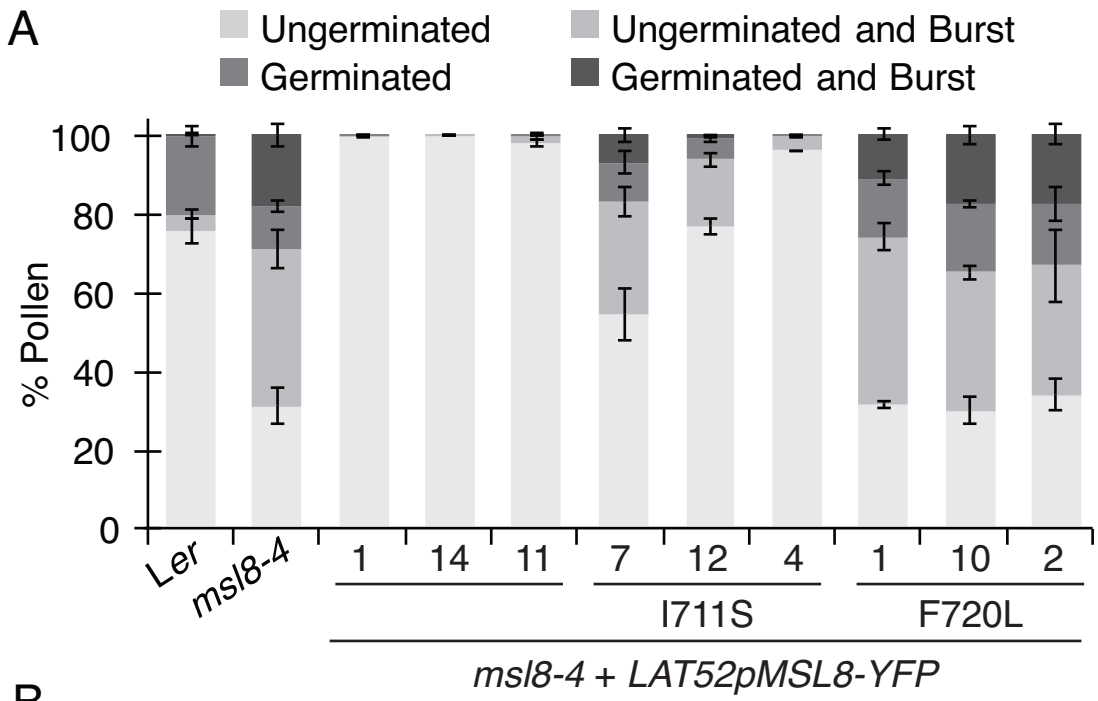
A
Ungerminated
Germinated
Ungerminated and Burst
Germinated and Burst
% Pollen
100
80
60
40
20
0
Ler
msl8-4
1
14
11
7
12
4
1
10
2
I711S
F720L
msl8-4 + LAT52pMSL8-YFP

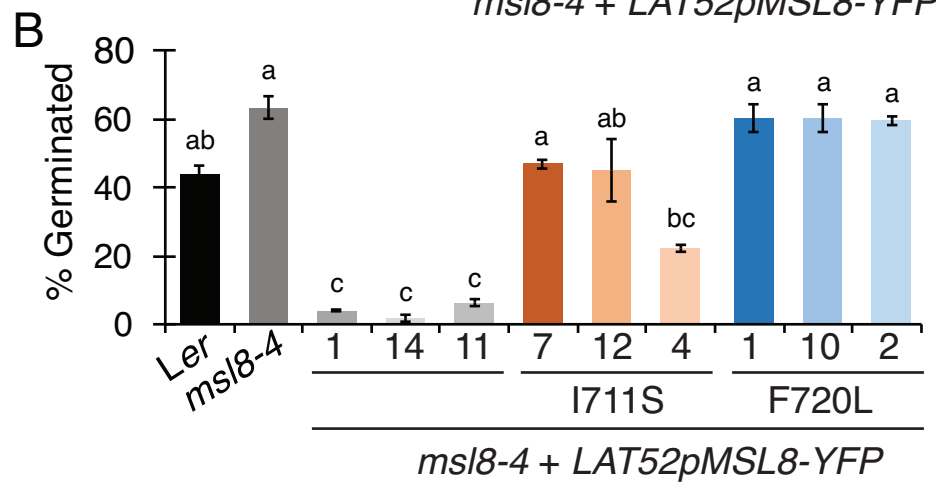
B
% Germinated
80
60
40
20
0
ab
a
c
c
c
a
ab
bc
a
a
a
Ler
msl8-4
1
14
11
7
12
4
1
10
2
I711S
F720L
msl8-4 + LAT52pMSL8-YFP

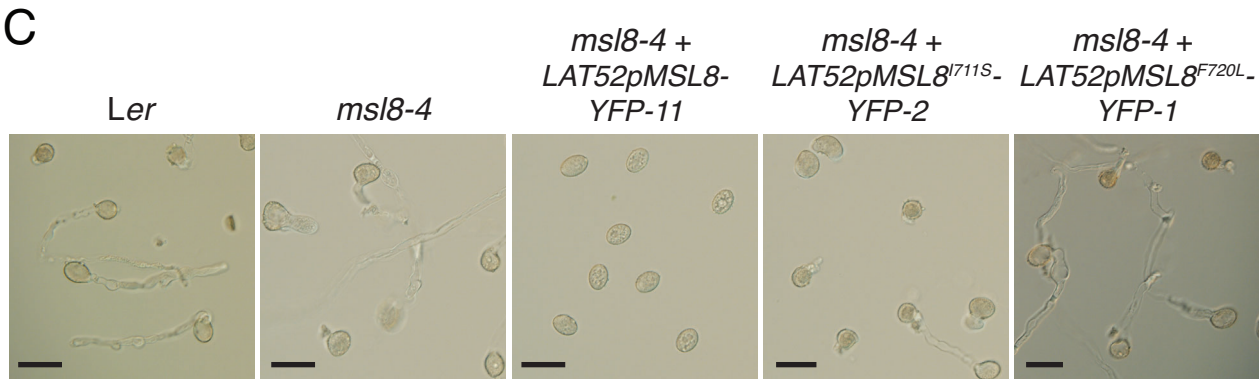
C
Ler
msl8-4
msl8-4 + LAT52pMSL8-YFP-11
msl8-4 + LAT52pMSL8I711S-YFP-2
msl8-4 + LAT52pMSL8F720L-YFP-1

FIGURE 8

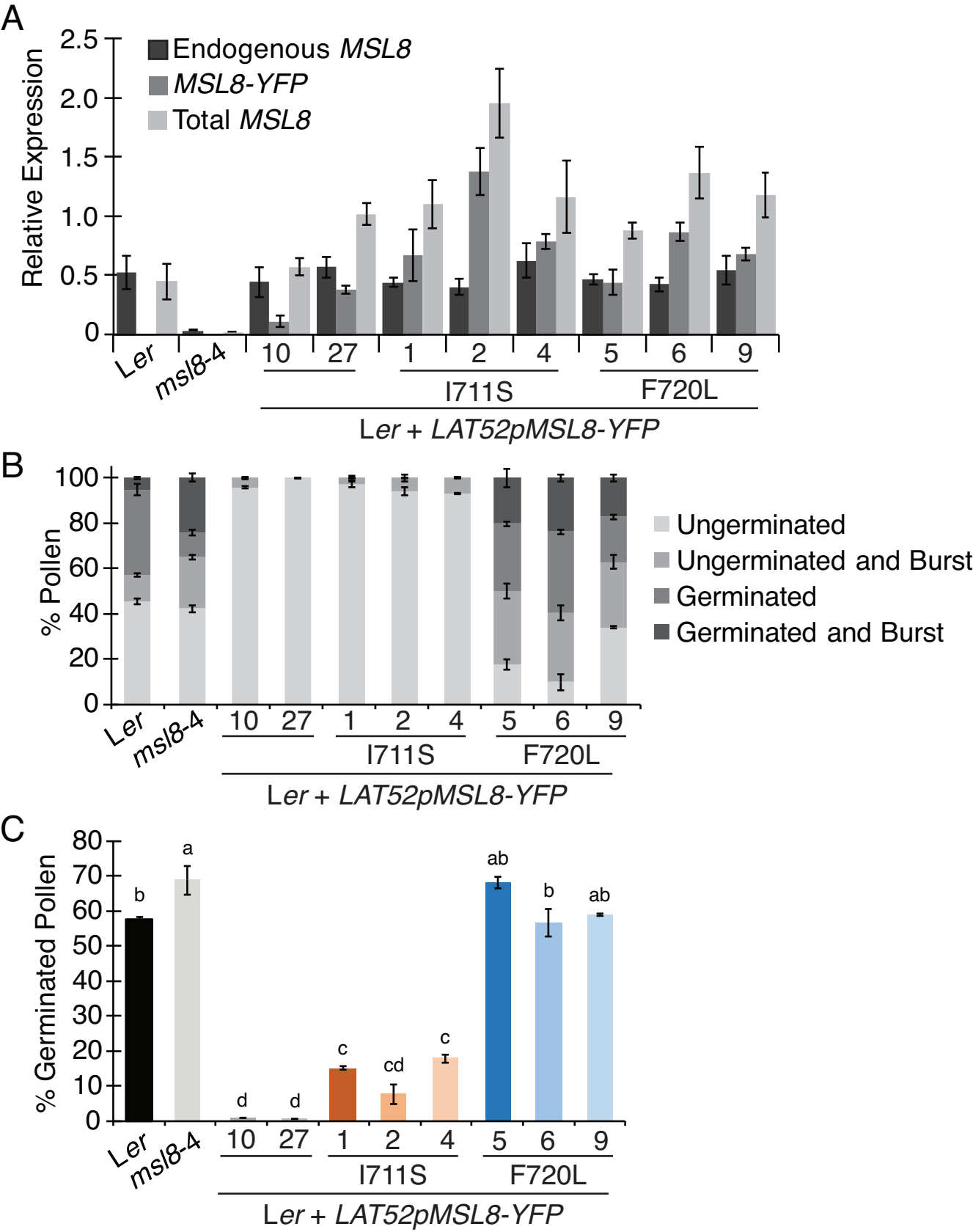
A
Relative Expression
2.5
2.0
1.5
1.0
0.5
0
Endogenous MSL8
MSL8-YFP
Total MSL8
Ler
msl8-4
10
27
1
2
4
5
6
9
I711S
F720L
Ler + LAT52pMSL8-YFP
B
% Pollen
100
80
60
40
20
0
Ungerminated
Ungerminated and Burst
Germinated
Germinated and Burst
Ler
msl8-4
10
27
1
2
4
5
6
9
I711S
F720L
Ler + LAT52pMSL8-YFP
C
% Germinated Pollen
80
70
60
50
40
30
20
10
0
b
a
d
d
c
cd
c
ab
b
ab
Ler
msl8-4
10
27
1
2
4
5
6
9
I711S
F720L
Ler + LAT52pMSL8-YFP

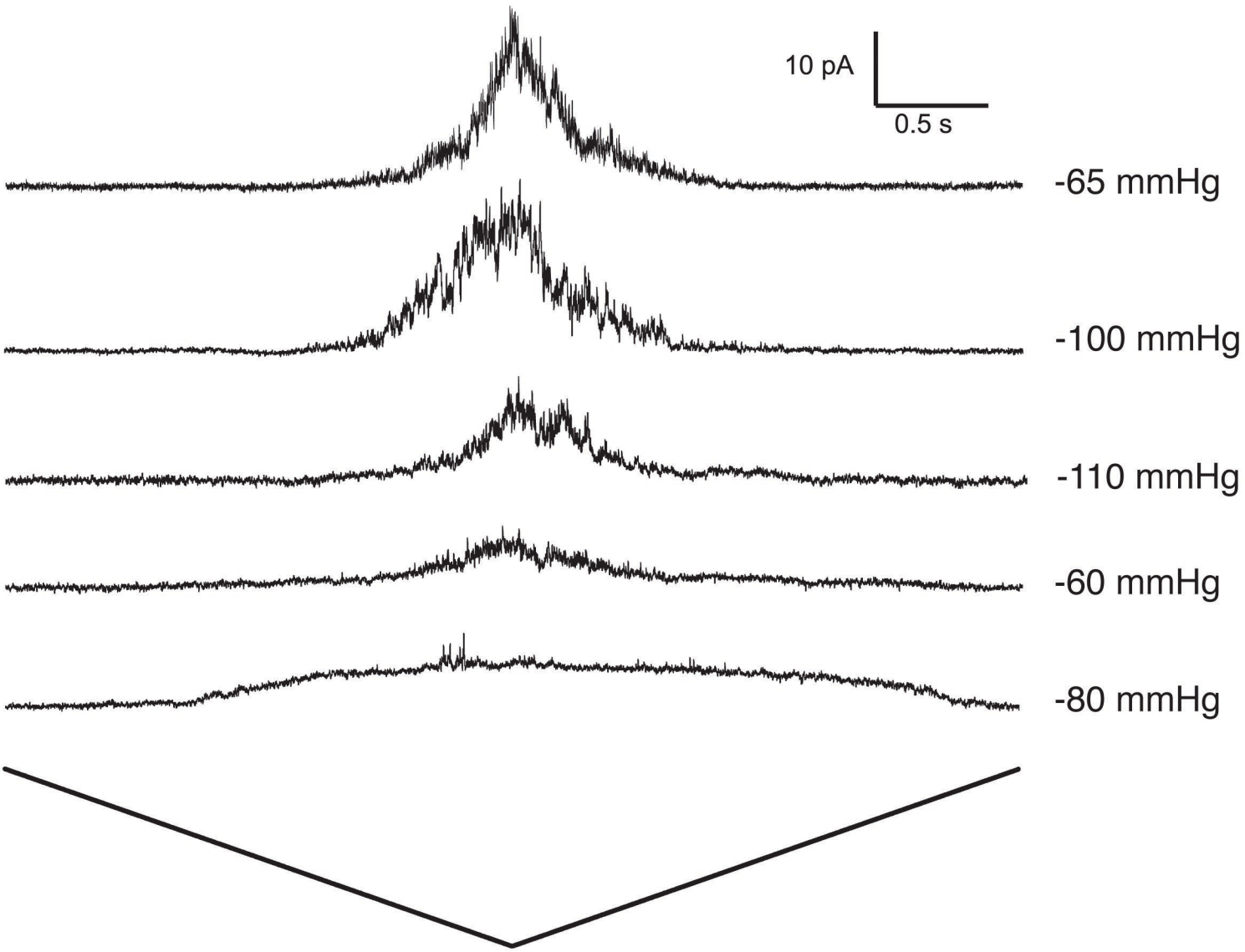

Supplementary Figure 1. Representative traces of MSL8^{F720L} expressed in *Xenopus laevis* oocytes. Representative traces from excised inside-out patches of plasma membrane from *Xenopus* oocytes 2 to 10 days following injection with *MSL8^{F720L}* cRNA clamped at -40 mV membrane potential. The peak suction applied during the pressure ramp is indicated next to each trace.

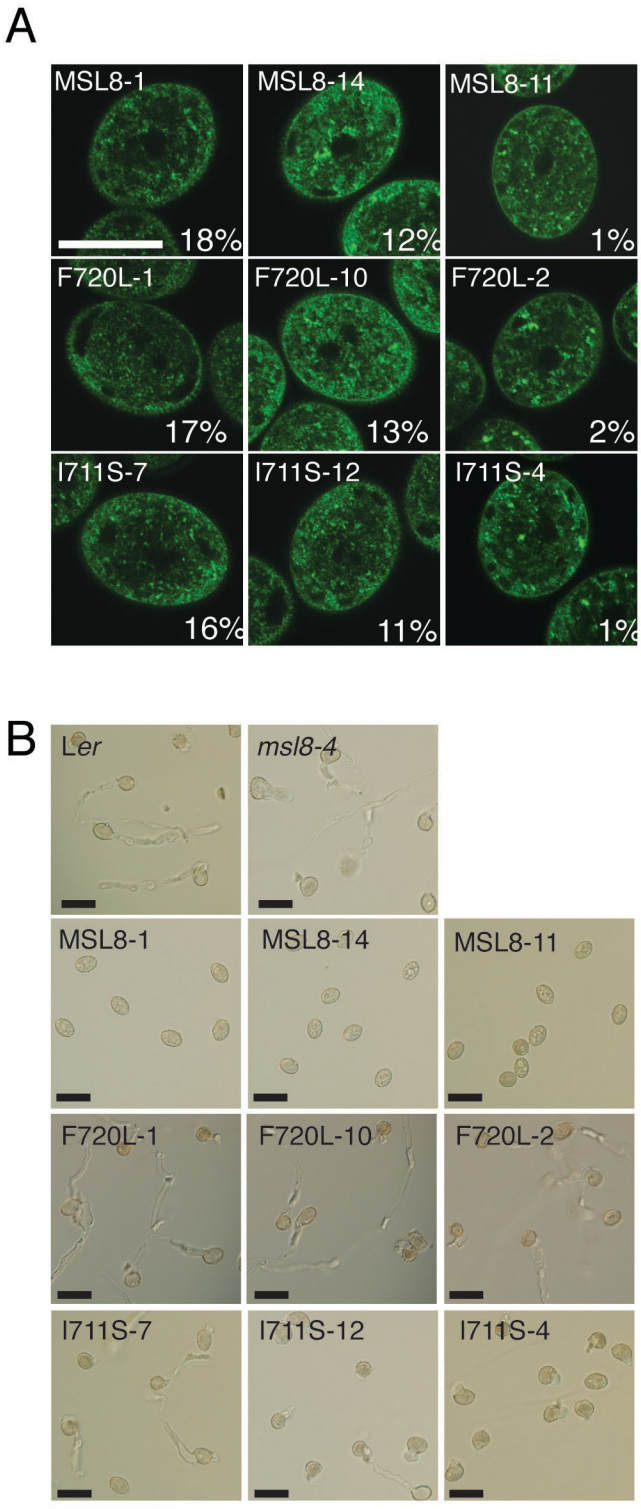

Supplementary Figure 2. Additional characterization of *msl8-4* pollen expressing *LAT52pMSL8-YFP* variants. (**A**) Confocal images of YFP signal in pollen from the indicated lines expressing *LAT52pMSL8-YFP* in the *msl8-4* background. The laser power at which images were collected is indicated in the lower right corner. All other imaging conditions were kept constant. Scale bars are 20 μm. (**B**) Pollen from the indicated lines incubated for 16 hours in liquid germination media. Scale bars are 50 μm.

Supplementary Figure 3. Alignment of the predicted pore-lining domain of Group III MSLs from *Arabidopsis thaliana*. Residues identical in at least half of the sequences are shaded in black; similar residues are shaded in gray. Arrowheads mark sites conserved in all sequences. White arrowhead marks Phe720.

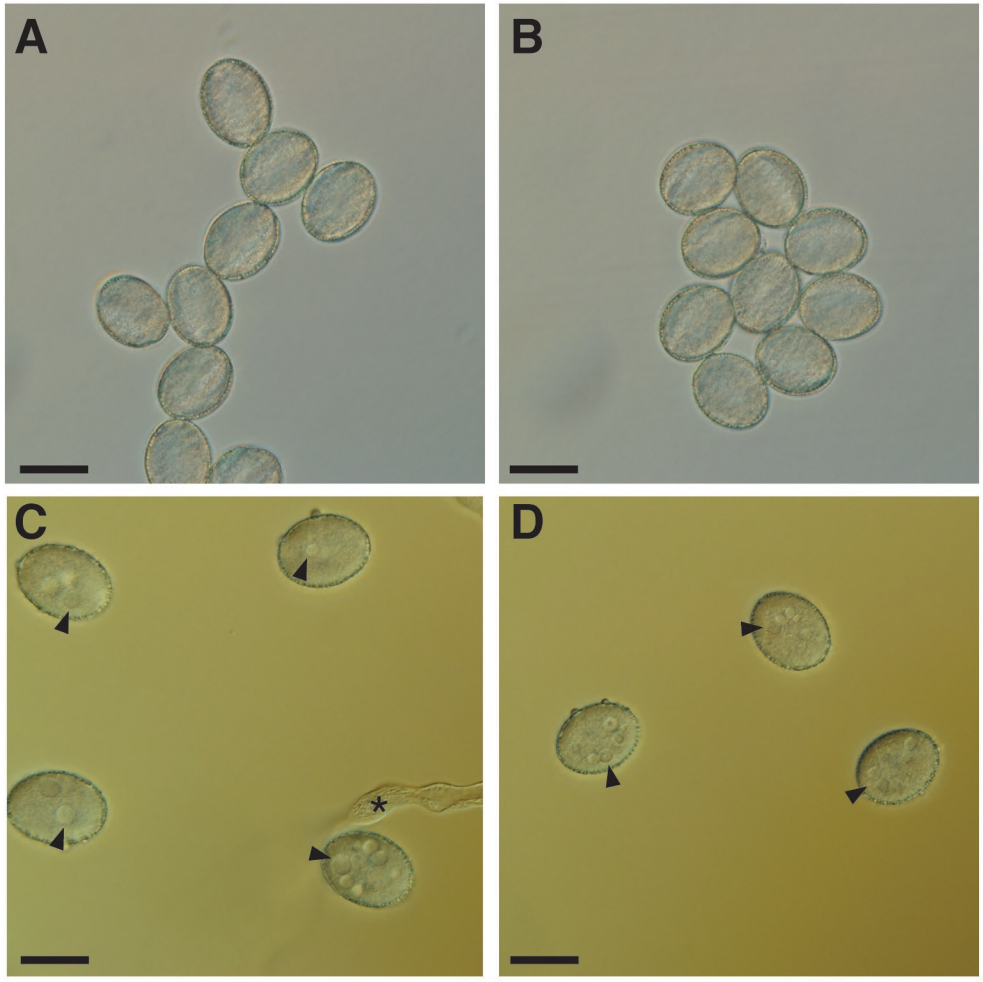

Supplementary Figure 4. Vacuolization of L*er* and *LAT52pMSL8-YFP*-expressing pollen during germination. Pollen incubated in germination media for approximately 5 minutes (**A**-**B**) or 6 hours (**C**-**D**). (**A**, **C**) L*er* pollen. (**B**, **D**) *msl8-4 + LAT52pMSL8-YFP-14* pollen. Arrowheads mark larger vacuoles found in pollen from both genotypes after extended incubation in germination media. Asterisk marks pollen tube. Scale bars are 20 μm.

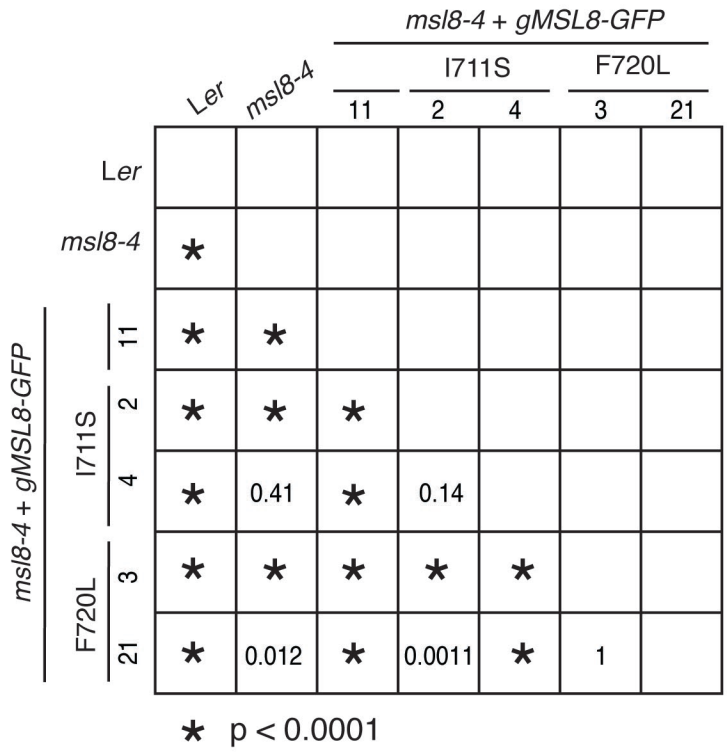

Supplementary Table 1. Statistical groupings of pollen germination and bursting rates in *msl8-4 + gMSL8-GFP* variant lines. Results of a chi-squared test comparing the pattern of ungerminated; ungerminated and burst; germinated; and germinated and burst pollen after incubation in pollen germination media for 6 hours. p-values were corrected using the Bonferroni method. Asterisks mark p-values less than 0.0001.

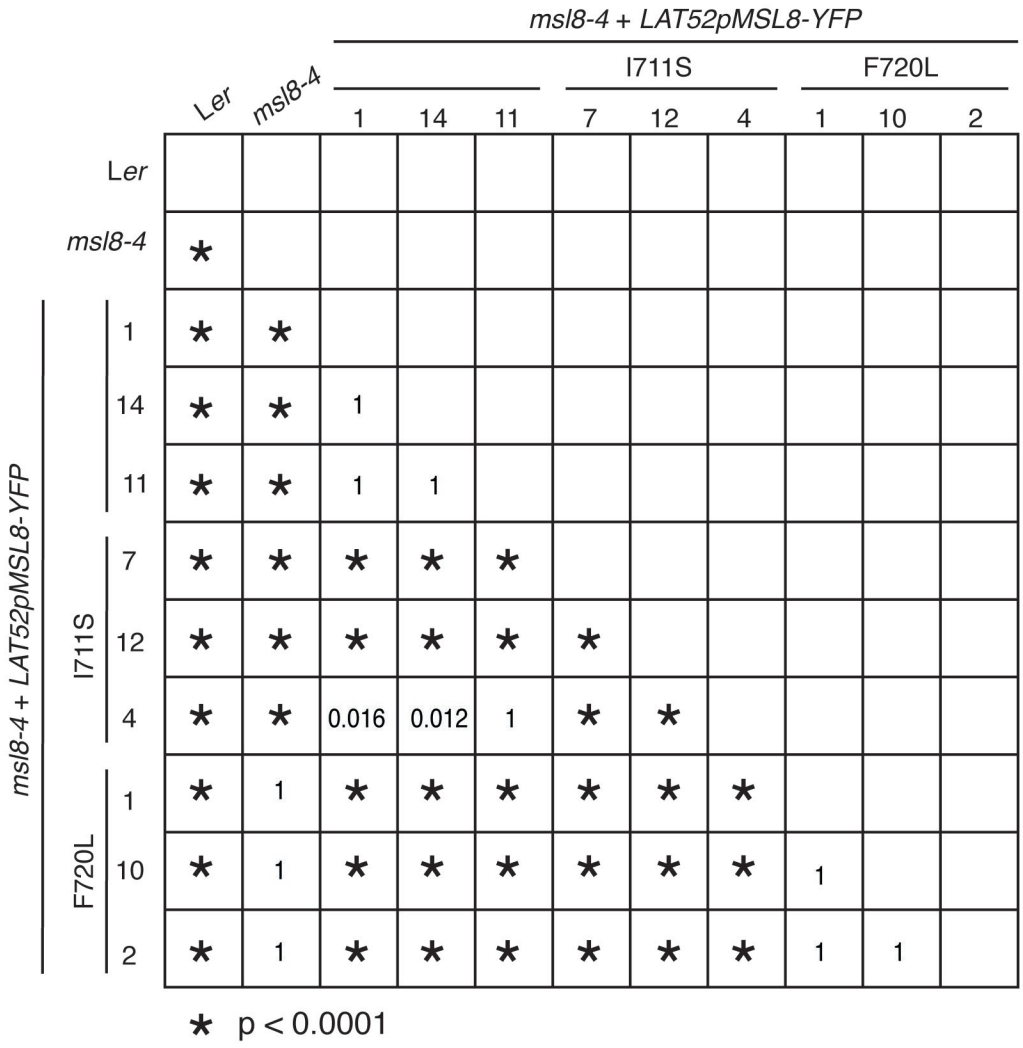

Supplementary Table 2. Statistical groupings of pollen germination and bursting rates in *msl8-4 + LAT52pMSL8-YFP* variant lines. Results of a chi-squared test comparing the pattern of ungerminated; ungerminated and burst; germinated; and germinated and burst pollen after incubation in pollen germination media for 6 hours. p-values were corrected using the Bonferroni method. Asterisks mark p-values less than 0.0001.

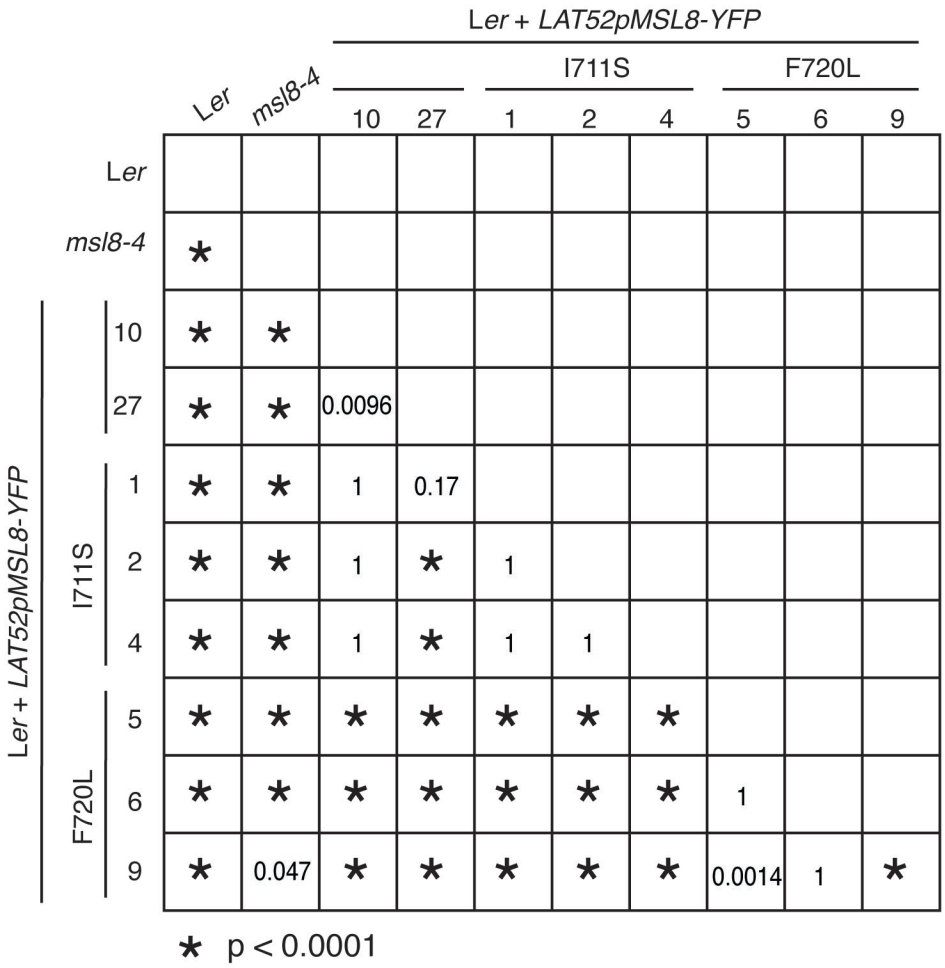

Supplementary Table 3. Statistical groupings of pollen germination and bursting rates in L*er* + *LAT52pMSL8-YFP* variant lines. Results of a chi-squared test comparing the pattern of ungerminated; ungerminated and burst; germinated; and germinated and burst pollen after incubation in pollen germination media for 6 hours. p-values were corrected using the Bonferroni method. Asterisks mark p-values less than 0.0001.

	RT-PCR	
	Forward	Reverse
ACTIN	5'-CAACCGGTATTGTGCTGGATTC-3'	5'-GATGGCATGAGGAAGAGAGAAAC-3'
		5'-GGATAGCATGAGGAAGAGCATAC-3'
		5'-GAGACGGAGGATAGCATGTG-3'
Total *MSL8*	5'-GCAATCGAGTTCTGTGTCCAC-3'	5'-CCAATACTCCGGCTTGTTGTCG-3'
Endogenous *MSL8*	5'-CGAACTACATCGACAACAAGCCG-3'	5'-GCAAAATGAAAAGTGTTGTGTTGTTCATC-3'
MSL8-YFP	5'-CTGGCTGGTCACAAAACCAAC-3'	5'-CTTGTGGCCGTTTACGTCG-3'

Supplementary Table 4. Primers used in quantitative reverse-transcriptase polymerase chain reactions.